Charged lepton flavor violation in supersymmetric low-scale seesaw models

Amon Ilakovac,[1] Apostolos Pilaftsis,[2] and Luka Popov[1]

[1]*University of Zagreb, Department of Physics, Bijenička cesta 32, P.O. Box 331, Zagreb, Croatia*
[2]*Consortium for Fundamental Physics, School of Physics and Astronomy, University of Manchester, Manchester M13 9PL, United Kingdom*

We study charged lepton flavor violation in low-scale seesaw models of minimal supergravity, which realize large neutrino Yukawa couplings thanks to approximate lepton-number symmetries. There are two dominant sources of lepton flavor violation in such models. The first source originates from the usual soft supersymmetry-breaking sector, whilst the second one is entirely supersymmetric and comes from the supersymmetric neutrino Yukawa sector. Within the framework of minimal supergravity, we consider both sources of lepton flavor violation, soft and supersymmetric, and calculate a number of possible lepton-flavor-violating transitions, such as the photonic decays of muons and taus, $\mu \to e\gamma$, $\tau \to e\gamma$ and $\tau \to \mu\gamma$, their neutrinoless three-body decays, $\mu \to eee$, $\tau \to eee$, $\tau \to \mu\mu\mu$, $\tau \to ee\mu$ and $\tau \to e\mu\mu$, and the coherent $\mu \to e$ conversion in nuclei. After taking into account the exclusion bounds placed by present experiments of lepton flavor violation, we derive combined theoretical limits on the universal heavy Majorana mass scale m_N and the light-to-heavy neutrino mixings. Supersymmetric low-scale seesaw models offer distinct correlated predictions for lepton-flavor-violating signatures, which might be discovered in current and projected experiments, such as MEG, COMET/PRISM, Mu2e, super-BELLE and LHCb.

I. INTRODUCTION

Neutrino oscillation experiments [1–4] have provided undisputed evidence of lepton flavor violation (LFV) in the neutrino sector, pointing towards physics beyond the Standard Model (SM). Recent reactor neutrino oscillation experiments [5] have shown that the angle θ_{13} of the Pontecorvo-Maki-Nakagawa-Sakata mixing matrix [6] is nonzero, thus hinting at a nontrivial neutrino-flavor structure and possibly at *CP* violation. Nevertheless, in spite of intense experimental searches [7–11], no evidence of LFV has been found yet in the charged lepton sector of the SM, implying conservation of the individual lepton numbers associated with the electron e, the muon μ and the tau τ. All past and current experiments were only able to report upper limits on observables of charged lepton flavor violation (CLFV).

Recently, the MEG Collaboration [7] has announced an improved upper limit on the branching ratio of the CLFV decay $\mu \to e\gamma$, with $B(\mu \to e\gamma) < 2.4 \times 10^{-12}$ at the 90% confidence level. As also shown in Table I, future experiments searching for the CLFV processes, $\mu \to e\gamma$, $\mu \to eee$, coherent $\mu \to e$ conversion in nuclei, $\tau \to e\gamma/\mu\gamma$, $\tau \to 3$ leptons and $\tau \to$ lepton + light meson, are expected to reach branching-ratio sensitivities to the level of 10^{-13} [12] (10^{-14} [13]), 10^{-16} [14] (10^{-17} [13]), 10^{-17} [15,16] (10^{-18} [13,17]), 10^{-9} [18,19], 10^{-10} [18] and 10^{-10} [18], respectively. The values in parentheses indicate the sensitivities that are expected to be achieved by the new generation CLFV experiments in the next decade. Most interestingly, the projected sensitivity for

$\mu \to eee$ and $\mu \to e$ conversion in nuclei is expected to increase by 5 and 6 orders of magnitude, respectively. Given that CLFV is forbidden in the SM, its observation would constitute a clear signature for new physics, thus rendering this field of investigations even more exciting.

Although forbidden in the SM, CLFV is a generic feature for most of its extensions. One such well-motivated extension is the so-called minimal supersymmetric Standard Model (MSSM) [20], where supersymmetry (SUSY) is softly broken at the 1–10 TeV scale for phenomenological reasons. The MSSM provides a quantum-mechanically stable solution to the gauge hierarchy problem and predicts rather accurate unification of the SM gauge couplings close to the grand unified theory (GUT) scale. If *R* parity is conserved, the lightest supersymmetric particle is stable and, if neutral, such as the neutralino, it could play the role of the dark matter (DM) in the Universe. Finally, the MSSM typically predicts a SM-like Higgs boson lighter than 135 GeV, in agreement with the recent observations for a 125 GeV Higgs boson, made by the ATLAS [21] and CMS [22] Collaborations.

In the MSSM with *R*-parity conservation, the lepton number is preserved and all left-handed light neutrinos $\nu_{e,\mu,\tau}$ remain massless, exactly as in the SM. To account for the observed light-neutrino masses and mixings, while maintaining *R* parity, the field content of the MSSM needs to be extended. An interesting extension to the MSSM is provided by the so-called seesaw mechanism. There are three realizations of the seesaw mechanism: the seesaw type I [23], the seesaw type II [24] and the seesaw type III [25]. The three scenarios differ by the nature of their

TABLE I. Current upper limits and future sensitivities of CLFV observables under study.

No.	Observable	Upper limit	Future sensitivity
1.	$B(\mu \to e\gamma)$	2.4×10^{-12} [7]	$1 - 2 \times 10^{-13}$ [12], 10^{-14} [13]
2.	$B(\mu \to eee)$	10^{-12} [8]	10^{-16} [14], 10^{-17} [13]
3.	$R_{\mu e}^{\mathrm{Ti}}$	4.3×10^{-12} [9]	$3 - 7 \times 10^{-17}$ [15,16], 10^{-18} [13,17]
4.	$R_{\mu e}^{\mathrm{Au}}$	7×10^{-13} [10]	$3 - 7 \times 10^{-17}$ [15,16], 10^{-18} [13,17]
5.	$B(\tau \to e\gamma)$	3.3×10^{-8} [11]	$1 - 2 \times 10^{-9}$ [18,19]
6.	$B(\tau \to \mu\gamma)$	4.4×10^{-8} [11]	2×10^{-9} [18,19]
7.	$B(\tau \to eee)$	2.7×10^{-8} [11]	2×10^{-10} [18,19]
8.	$B(\tau \to e\mu\mu)$	2.7×10^{-8} [11]	10^{-10} [18]
9.	$B(\tau \to \mu\mu\mu)$	2.1×10^{-8} [11]	2×10^{-10} [18,19]
10.	$B(\tau \to \mu ee)$	1.8×10^{-8} [11]	10^{-10} [18]

seesaw messengers that are needed to explain the small neutrino masses. In this study, we will adopt a low-scale variant of the seesaw type-I realization, whose messengers are three singlet heavy neutrinos $N_{1,2,3}$.

In the usual seesaw type-I mechanism, the heavy singlet neutrinos must assume masses of order $\sim 10^{12-14}$ GeV, for electroweak-scale Dirac neutrino masses, in order to account for the observed light-neutrino mass spectrum. The mixing between light and heavy neutrinos is of the order $\xi_{\nu N} \sim \sqrt{m_\nu/m_N} \sim 10^{-12}$, for light-neutrino masses $m_\nu \sim 10^{-1}$ eV. As a consequence, heavy neutrinos decouple from low-energy processes of CLFV in the SM with right-handed neutrinos, giving rise to extremely suppressed and unobservable rates. In the MSSM with right-handed neutrinos, however, the singlet heavy neutrinos do not fully decouple. They impact the low-energy sector, through renormalization group (RG) effects that induce sizeable LFV in the slepton sector for a SUSY mass scale $M_{\mathrm{SUSY}} \sim 1$–10 TeV.

A potentially interesting alternative to the ordinary seesaw mechanism may arise from the presence of approximate lepton-number symmetries [26–29] in the theory. The smallness of the light-neutrino masses is a consequence of these approximate leptonic symmetries which are radiatively stable [29,30], whilst the heavy neutrino mass scale could be as low as 100 GeV. Unlike in the usual seesaw scenario, the light-to-heavy neutrino mixings $\xi_{\nu N}$ are not correlated to the light-neutrino masses m_ν. Instead, $\xi_{\nu N}$ are free parameters, constrained by experimental limits on deviations of the $W^\pm$- and Z-boson couplings to leptons with respect to their SM values [31,32]. Approximate lepton-number symmetries do not restrict the size of LFV, and so potentially large phenomena of CLFV may be predicted. This feature is quite generic both in the SM [33] and in the MSSM [34,35] augmented with low-scale right-handed neutrinos. It is this new source for LFV in the MSSM that we wish to study in detail here, in addition to the one resulting from the frequently considered soft SUSY-breaking sector [36–39].

In this article, we denote for brevity the SM and the MSSM extended by low-scale right-handed neutrinos and

approximate lepton-number symmetries by ν_RSM and ν_RMSSM, respectively. Our study in this paper focuses on the ν_RMSSM with constrained boundary conditions at the gauge-coupling unification scale, within the framework of minimal supergravity (mSUGRA). However, the results presented here are applicable to more general soft SUSY-breaking scenarios.

The ν_RMSSM has some interesting features with respect to the MSSM. In particular, the heavy singlet sneutrinos may emerge as new viable candidates of cold dark matter [40]. In addition, the mechanism of low-scale resonant leptogenesis [30,41] could provide a possible explanation for the observed Baryon asymmetry in the Universe, as the parameter space for successful electroweak baryogenesis gets squeezed by the current LHC data [42].

Given the multitude of quantum states mediating LFV in the ν_RMSSM, the predicted values for observables of CLFV in this model turn out to be generically larger than the corresponding ones in the ν_RSM, except possibly for $B(l \to l'\gamma)$ [34,35], where $l, l' = e, \mu, \tau$. The origin of suppression for the latter branching ratios may partially be attributed to the SUSY no-go theorem due to Ferrara and Remiddi [43], which states that the magnetic dipole moment operator necessarily violates SUSY and it has therefore to vanish in the supersymmetric limit of the theory.

The goal of this paper is to improve upon earlier calculations of CLFV in supersymmetric low-scale seesaw models which are either approximate, or incomplete. Specifically, in Ref. [34] a low-scale aligned neutrino and sneutrino spectrum was assumed to the leading order in the heavy neutrino mass, whilst in Refs. [44,45] only a subset of loop effects mediated by the photon γ, the Z boson, the neutral Higgs scalars and box graphs was considered. Instead, we present here detailed analytical expressions for CLFV observables, induced by γ- and Z-boson form factors, as well as the *complete* set of box contributions involving heavy neutrinos, sleptons, sneutrinos, charginos, neutralinos and charged Higgs bosons. We also derive the complete set of kinematic form factors that contributes to the three-body LFV decays of the muon and tau, such as $\mu \to eee$, $\tau \to eee$, $\tau \to \mu\mu\mu$, $\tau \to ee\mu$ and $\tau \to e\mu\mu$.

In our numerical analysis, we consider benchmark scenarios of the ν_RMSSM, which are in agreement with the existing LHC data from the recent discovery of a SM-like Higgs boson [21,22] and the nonobservation of squarks and gluinos [46].

The paper is organized as follows. In Sec. II we describe the relevant leptonic sector of the ν_RMSSM and introduce two baseline scenarios based on approximate lepton-number symmetries. Section III contains details of the calculation of the LFV amplitudes and branching ratios of CLFV decays of the tau and muon, where the complete set of chiral structures of the amplitudes contributing to the CLFV processes $l \to l'\gamma$, $l \to l'l_1\bar{l}_2$ and $\mu \to e$ conversion in nuclei are derived. Section IV presents numerical estimates for the aforementioned processes of CLFV, within the two baseline mSUGRA scenarios introduced in Sec. II. Moreover, we discuss correlated predictions of the CLFV observables with $B(l \to l'\gamma)$ and other kinematic parameters. Section V summarizes the results of our analysis and presents our conclusions. All technical details have been relegated to the appendices. In Appendix A, we give all relevant interaction vertices in the ν_RMSSM. Appendix B defines the one-loop functions that appear in our analytic calculations. In terms of these loop functions, Appendix C describes the analytic results for all the one-loop form factors that occur in the CLFV transition amplitudes.

II. LOW-SCALE SEESAW MODELS AND LEPTON FLAVOR VIOLATION

In this section we describe the leptonic sector of the MSSM extended by low-scale right-handed neutrinos, which we call the ν_RMSSM for brevity. In addition, we introduce the neutrino Yukawa structure of two baseline scenarios based on approximate lepton-number symmetries and universal Majorana masses at the GUT scale. We will use these two scenarios to present generic predictions of CLFV within the framework of mSUGRA.

The leptonic superpotential part of the ν_RMSSM reads

$$W_{\text{lepton}} = \hat{E}^C \mathbf{h}_e \hat{H}_d \hat{L} + \hat{N}^C \mathbf{h}_\nu \hat{L} \hat{H}_u + \frac{1}{2} \hat{N}^C \mathbf{m}_M \hat{N}^C, \quad (2.1)$$

where $\hat{H}_{u,d}$, $\hat{L}$, $\hat{E}$ and $\hat{N}^C$ denote the two Higgs-doublet superfields, the three left- and right-handed charged lepton superfields and the three right-handed neutrino superfields, respectively. The Yukawa couplings $\mathbf{h}_{e,\nu}$ and the Majorana mass parameters $\mathbf{m}_M$ form 3×3 complex matrices. Here, the Majorana mass matrix $\mathbf{m}_M$ is taken to be SO(3)-symmetric at the GUT scale, i.e. $\mathbf{m}_M = m_N \mathbf{1}_3$.

In this study, we consider low-scale seesaw models [26–29], where the smallness of the light-neutrino masses is protected by natural, quantum-mechanically stable cancellations due to the presence of approximate leptonic symmetries [29], whilst the Majorana mass scale m_N can be as low as 100 GeV. In these models, the neutrino induced LFV transitions from a charged lepton $l = \mu, \tau$

to another charged lepton $l' \neq l$ are functions of the ratios [33,47,48]

$$\mathbf{\Omega}_{l'l} = \frac{v_u^2}{2m_N^2}(\mathbf{h}_\nu^\dagger \mathbf{h}_\nu)_{l'l} = \sum_{i=1}^{3} B_{l'N_i} B_{lN_i}, \quad (2.2)$$

and are not constrained by the usual seesaw factor m_ν/m_N, where $v_u/\sqrt{2} \equiv \langle H_u \rangle$ is the vacuum expectation value (VEV) of the Higgs doublet H_u, with $\tan\beta \equiv \langle H_u \rangle/\langle H_d \rangle$. Moreover, the mixing matrix B_{lN_i} that occurs in the interaction of the $W^\pm$ bosons with the charged leptons $l = e, \mu, \tau$ and the three heavy neutrinos $N_{1,2,3}$ is defined in Appendix A. Note that the LFV parameters $\Omega_{l'l}$ do not directly depend on the RG evolution of the soft SUSY-breaking parameters, except through the VEV v_u at the minimum of the Higgs potential.

In the weak basis $\{(\nu_{e,\mu,\tau L})^C, \nu_{1,2,3R}\}$, the neutrino mass matrix in the ν_RMSSM takes on the standard seesaw type-I form [23]:

$$\mathbf{M}_\nu = \begin{pmatrix} 0 & \mathbf{m}_D \\ \mathbf{m}_D^T & \mathbf{m}_M^* \end{pmatrix}, \quad (2.3)$$

where $\mathbf{m}_D = \sqrt{2}M_W \sin\beta\, g_w^{-1} \mathbf{h}_\nu^\dagger$ and $\mathbf{m}_M$ are the Dirac- and Majorana-neutrino mass matrices, respectively. In this paper, we consider two baseline scenarios of neutrino Yukawa couplings. The first one realizes a U(1) leptonic symmetry [30] and is given by

$$\mathbf{h}_\nu = \begin{pmatrix} 0 & 0 & 0 \\ ae^{-\frac{i\pi}{4}} & be^{-\frac{i\pi}{4}} & ce^{-\frac{i\pi}{4}} \\ ae^{\frac{i\pi}{4}} & be^{\frac{i\pi}{4}} & ce^{\frac{i\pi}{4}} \end{pmatrix}. \quad (2.4)$$

In the second scenario, the structure of the neutrino Yukawa matrix $\mathbf{h}_\nu$ is motivated by the discrete symmetry group A_4 and has the following form [49]:

$$\mathbf{h}_\nu = \begin{pmatrix} a & b & c \\ ae^{-\frac{2\pi i}{3}} & be^{-\frac{2\pi i}{3}} & ce^{-\frac{2\pi i}{3}} \\ ae^{\frac{2\pi i}{3}} & be^{\frac{2\pi i}{3}} & ce^{\frac{2\pi i}{3}} \end{pmatrix}. \quad (2.5)$$

In (2.4) and (2.5), the Yukawa parameters a, b and c are assumed to be real. If the above leptonic (discrete or continuous) symmetries are not broken, the light-neutrinos are massless. The neutrino masses are obtained by adding small terms that break the symmetry of the Yukawa matrix. It is essential to remark here that the predictions for CLFV are independent of the flavor structure of these small symmetry-breaking terms in our low-scale seesaw models under study. These terms are needed to fit the low-energy neutrino data. For this reason, we do not discuss here particular symmetry breaking patterns of the above two baseline Yukawa scenarios given in (2.4) and (2.5).

The second source of LFV in the models under consideration originates from scalar-neutrino (sneutrino) interactions, namely the supersymmetric partners of the left-handed and right-handed neutrinos. Specifically, the sneutrino mass Lagrangian in flavor and mass bases is given by

$$\mathcal{L}^{\tilde{\nu}} = (\tilde{\nu}_L^\dagger, \tilde{\nu}_R^{C\dagger}, \tilde{\nu}_L^T, \tilde{\nu}_R^{CT}) \mathbf{M}_{\tilde{\nu}}^2 \begin{pmatrix} \tilde{\nu}_L \\ \tilde{\nu}_R^C \\ \tilde{\nu}_L^* \\ \tilde{\nu}_R^{C*} \end{pmatrix}$$

$$= \tilde{N}^\dagger \mathcal{U}^{\tilde{\nu}\dagger} \mathbf{M}_{\tilde{\nu}}^2 \mathcal{U}^{\tilde{\nu}} \tilde{N} = \tilde{N}^\dagger \hat{\mathbf{M}}_{\tilde{\nu}}^2 \tilde{N}, \qquad (2.6)$$

where $\mathbf{M}_{\tilde{\nu}}^2$ is a 12×12 Hermitian mass matrix in the flavor basis and $\hat{\mathbf{M}}_{\tilde{\nu}}^2$ is the corresponding diagonal mass matrix in the mass basis. More explicitly, in the flavor basis $\{\tilde{\nu}_{e,\mu,\tau L}, \tilde{\nu}_{1,2,3R}^C, \tilde{\nu}_{e,\mu,\tau L}^*, \tilde{\nu}_{1,2,3R}^{C*}\}$, the sneutrino mass matrix $\mathbf{M}_{\tilde{\nu}}^2$ may be cast into the form

$$\mathbf{M}_{\tilde{\nu}}^2 = \begin{pmatrix} \mathbf{H}_1 & \mathbf{N} & \mathbf{0} & \mathbf{M} \\ \mathbf{N}^\dagger & \mathbf{H}_2^T & \mathbf{M}^T & \mathbf{0} \\ \mathbf{0} & \mathbf{M}^* & \mathbf{H}_1^T & \mathbf{N}^* \\ \mathbf{M}^\dagger & \mathbf{0} & \mathbf{N}^T & \mathbf{H}_2 \end{pmatrix}, \qquad (2.7)$$

where the block entries are the following 3×3 matrices:

$$\begin{aligned} \mathbf{H}_1 &= \mathbf{m}_{\tilde{L}}^2 + \mathbf{m}_D \mathbf{m}_D^\dagger + \frac{1}{2} M_Z^2 \cos 2\beta, \\ \mathbf{H}_2 &= \mathbf{m}_{\tilde{\nu}}^2 + \mathbf{m}_D^\dagger \mathbf{m}_D + \mathbf{m}_M \mathbf{m}_M^\dagger, \\ \mathbf{M} &= \mathbf{m}_D(\mathbf{A}_\nu - \mu \cot \beta), \\ \mathbf{N} &= \mathbf{m}_D \mathbf{m}_M. \end{aligned} \qquad (2.8)$$

Here $\mathbf{m}_{\tilde{L}}^2$, $\mathbf{m}_{\tilde{\nu}}^2$ and $\mathbf{A}_\nu$ are 3×3 soft SUSY-breaking matrices associated with the left-handed slepton doublets, the right-handed sneutrinos and their trilinear couplings, respectively. In the supersymmetric limit, all the soft SUSY-breaking matrices are equal to zero, $\tan \beta = 1$ and $\mu = 0$. As a consequence, the sneutrino mass matrix $\mathbf{M}_{\tilde{\nu}}^2$ can be expressed in terms of the neutrino mass matrix $\mathbf{M}_\nu$ in (2.3) as follows:

$$\mathbf{M}_{\tilde{\nu}}^2 \overset{\text{SUSY}}{\to} \begin{pmatrix} \mathbf{M}_\nu \mathbf{M}_\nu^\dagger & \mathbf{0}_{6\times 6} \\ \mathbf{0}_{6\times 6} & \mathbf{M}_\nu^\dagger \mathbf{M}_\nu \end{pmatrix}, \qquad (2.9)$$

leading to the expected equality between neutrino and sneutrino mixings. Sneutrino LFV mixings do depend on the RG evolution of the ν_RMSSM parameters, but unlike the LFV mixings induced by soft SUSY-breaking terms, the sneutrino LFV mixings do not vanish at the GUT scale.

The sneutrino LFV mixings are obtained as combinations of unitary matrices that diagonalize the sneutrino, slepton and chargino mass matrices. It is interesting to notice that in the diagonalization of the sneutrino mass matrix $\mathbf{M}_{\tilde{\nu}}^2$ in (2.7), the sneutrino fields $\tilde{\nu}_{e,\mu,\tau L}$, $\tilde{\nu}_{1,2,3R}^C$ and their complex conjugates $\tilde{\nu}_{e,\mu,\tau L}^*$, $\tilde{\nu}_{1,2,3R}^{C*}$ are treated independently. As a result, the expressions for $\tilde{\nu}_{e,\mu,\tau L}$ and $\tilde{\nu}_{1,2,3R}^C$, in terms of the real-valued mass eigenstates $\tilde{N}_{1,2,\dots,12}$, are not manifestly complex conjugates to $\tilde{\nu}_{e,\mu,\tau L}^*$ and $\tilde{\nu}_{1,2,3R}^{C*}$, thus leading to a twofold interpretation of the flavor basis fields,

$$\tilde{\nu}_i^* = (\tilde{\nu}_i)^* = \mathcal{U}_{iA}^{\tilde{\nu}*} \tilde{N}_A, \qquad \tilde{\nu}_i^* = \mathcal{U}_{i+6A}^{\tilde{\nu}} \tilde{N}_A, \qquad (2.10)$$

where $\tilde{\nu}_{1,2,3} \equiv \tilde{\nu}_{e,\mu,\tau L}$ and $\tilde{\nu}_{4,5,6} \equiv \tilde{\nu}_{1,2,3R}^C$, with $i = 1, 2, \dots, 6$ and $A = 1, 2, \dots, 12$. For this reason, in Appendix A we include all equivalent forms that the Lagrangians, such as $\mathcal{L}_{\tilde{e}\tilde{\chi}^-\tilde{N}}$ and $\mathcal{L}_{\tilde{N}\tilde{N}Z}$, can be written down.

One technical comment is now in order. Unlike [34,35], the diagonalization of the 12×12 sneutrino mass matrix $\mathbf{M}_{\tilde{\nu}}^2$ and the resulting interaction vertices are evaluated numerically, without approximations. To perform the diagonalization of $\mathbf{M}_{\tilde{\nu}}^2$ numerically, we use the method developed in Ref. [50] for the neutrino mass matrix. This method becomes very efficient, if the diagonal submatrices have eigenvalues larger than the eigenvalues of the other submatrices. Therefore, we assume that the heavy neutrino mass scale m_N is of the order of, or larger than the scale of the other mass parameters in the ν_RMSSM.

Finally, a third source of LFV in the ν_RMSSM results from soft SUSY-breaking LFV terms. These LFV terms are induced by RG running and are absent at the GUT scale in mSUGRA. Their size strongly depends on the interval of the RG evolution from the GUT scale to the universal heavy neutrino mass scale m_N.

All the three different mechanisms of LFV, mediated by heavy neutrinos, heavy sneutrinos and soft SUSY-breaking terms, depend explicitly on the neutrino Yukawa matrix $\mathbf{h}_\nu$ and vanish in the limit $\mathbf{h}_\nu \to 0$.

III. CHARGED LEPTON FLAVOR VIOLATION

In this section, we present key details of our calculations for a number of CLFV observables in the ν_RMSSM. In detail, Sec. III A gives analytical results for the amplitudes of the CLFV decays: $l \to l'\gamma$ and $Z \to ll'^C$, and their branching ratios. Correspondingly, Secs. III B and III C give analytical expressions for the neutrinoless three-body decays $l \to l'l_1 l_2^C$ pertinent to muon and tau decays, and for coherent $\mu \to e$ conversion in nuclei. All these analytical results are expressed in terms of one-loop functions and composite form factors that are defined in Appendices B and C.

A. The decays $l \to l'\gamma$ and $Z \to ll'^C$

At the one-loop level, the effective couplings $\gamma l'l$ and $Zl'l$ are generated by the Feynman graphs shown in Fig. 1. The general form of the transition amplitudes associated with these effective couplings is given by

$$\begin{aligned} \mathcal{T}_\mu^{\gamma l'l} &= \frac{e\alpha_w}{8\pi M_W^2} \bar{l}' [(F_\gamma^L)_{l'l}(q^2\gamma_\mu - \slashed{q}q_\mu)P_L \\ &\quad + (F_\gamma^R)_{l'l}(q^2\gamma_\mu - \slashed{q}q_\mu)P_R + (G_\gamma^L)_{l'l}i\sigma_{\mu\nu}q^\nu P_L \\ &\quad + (G_\gamma^R)_{l'l}i\sigma_{\mu\nu}q^\nu P_R]l, \end{aligned} \qquad (3.1)$$

$$\mathcal{T}_\mu^{Zl'l} = \frac{g_w\alpha_w}{8\pi \cos\theta_w} \bar{l}'[(F_Z^L)_{l'l}\gamma_\mu P_L + (F_Z^R)_{l'l}\gamma_\mu P_R]l, \quad (3.2)$$

where $P_{L(R)} = \frac{1}{2}[1 - (+)\gamma_5]$, $\alpha_w = g_w^2/(4\pi)$, e is the electromagnetic coupling constant, $M_W = g_w\sqrt{v_u^2 + v_d^2}/2$ is
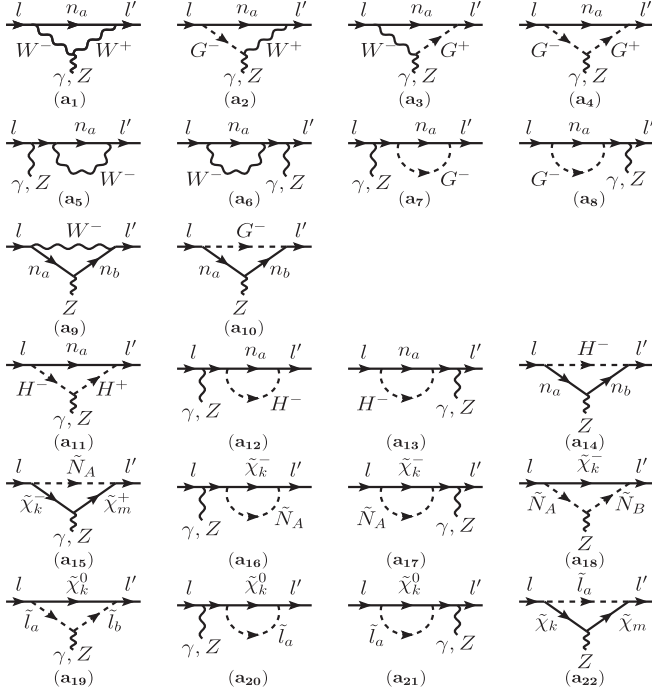
FIG. 1. Feynman graphs contributing to $l \to l' \gamma$ and $Z \to l^C l'$ ($l \to Zl'$) amplitudes.

$+ (l' \leftrightarrow l_1)$

FIG. 2. Feynman graphs contributing to the box $l \to l' l_1 l_2^C$ amplitudes.

the W-boson mass, θ_w is the weak mixing angle and $q = p_{l'} - p_l$ is the photon momentum. The form factors $(F_\gamma^L)_{l'l}$, $(F_\gamma^R)_{l'l}$ $(G_\gamma^L)_{l'l}$, $(G_\gamma^R)_{l'l}$, $(F_Z^L)_{l'l}$ and $(F_Z^R)_{l'l}$ receive contributions from heavy neutrinos $N_{1,2,3}$, heavy sneutrinos $\tilde{N}_{1,2,3}$ and RG induced soft SUSY-breaking terms. The analytical expressions for these three individual contributions are given in Appendix C. Note that according to our normalization, the composite form factors $(G_\gamma^L)_{l'l}$ and $(G_\gamma^R)_{l'l}$ have dimensions of mass, whilst all other form factors are dimensionless.

It is essential to remark here that the transition amplitudes (3.1) and (3.2) are also constituent parts of the leptonic amplitudes $l \to l' l_1 l_2^C$ and semileptonic amplitudes $l \to l' q_1 \bar{q}_2$, which will be discussed in more detail in Secs. III B and III C. To calculate the CLFV decay $l \to l' \gamma$, we only need to consider the dipole moment operators associated with the form factors $(G_\gamma^L)_{l'l}$ and $(G_\gamma^R)_{l'l}$ in (3.1). Taking this last fact into account, the branching ratios for $l \to l' \gamma$ and $Z \to l l'^C + l^C l'$ are given by

$$B(l \to l' \gamma) = \frac{\alpha_w^3 s_w^2}{256\pi^2} \frac{m_l^3}{M_W^4 \Gamma_l}(|(G_\gamma^L)_{l'l}|^2 + |(G_\gamma^R)_{l'l}|^2), \quad (3.3)$$

$$B(Z \to l' l^C + l'^C l) = \frac{\alpha_w^3 M_W}{768\pi^2 c_w^3 \Gamma_Z}(|(F_Z^L)_{l'l}|^2 + |(F_Z^R)_{l'l}|^2). \quad (3.4)$$

Observe that the above expressions are valid to leading order in external charged lepton masses and external momenta, which constitutes an excellent approximation
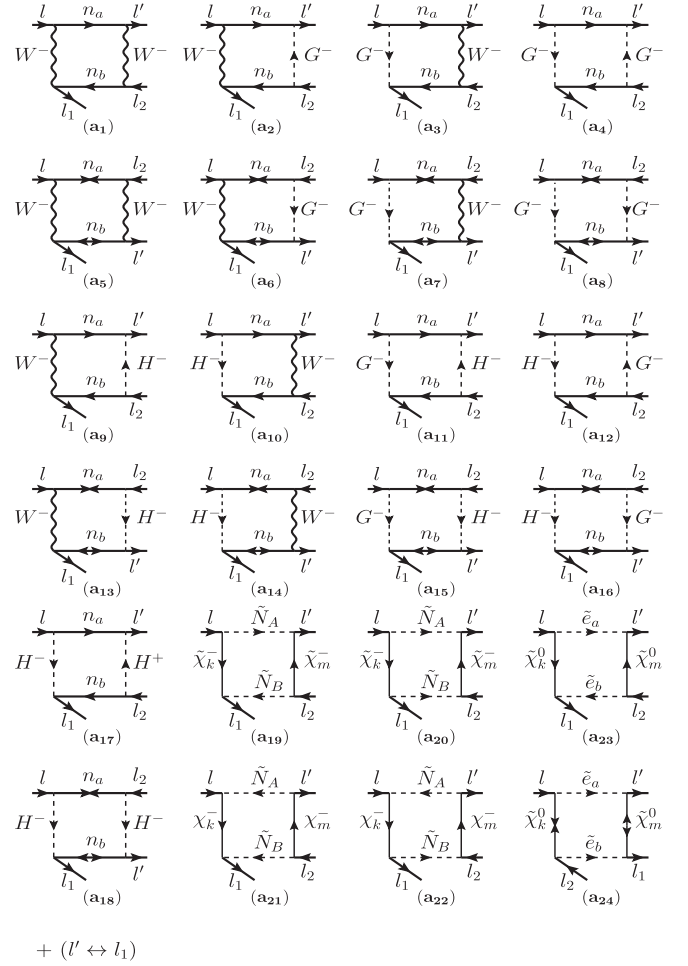
for our purposes. Thus, in (3.4) we have assumed that the Z-boson mass M_Z is much smaller than the SUSY and heavy neutrino mass scales, M_{SUSY} and m_N, and we have kept the leading term in an expansion of small momenta and masses for the external particles. In the decoupling regime of all soft SUSY-breaking and charged Higgs-boson masses, the low-energy sector of the ν_RMSSM becomes the ν_RSM. In this ν_RSM limit of the theory, the analytical expressions for $B(l \to l' \gamma)$ and $B(Z \to l' l^C + l'^C l)$ take on the forms presented in Refs. [47,51], respectively.

B. Three-body leptonic decays $l \to l' l_1 l_2^C$

We now study the three-body CLFV decays $l \to l' l_1 l_2^C$, where l can be the muon or tau, and l', l_1, l_2 denote other charged leptons to which l is allowed to decay kinematically.

The transition amplitude for $l \to l' l_1 l_2^C$ receives contributions from γ- and Z-boson-mediated graphs shown in Fig. 1 and from box graphs displayed in Fig. 2. The amplitudes for these three contributions are

$$\mathcal{T}_{\gamma}^{ll'l_1l_2} = \frac{\alpha_w^2 s_w^2}{2M_W^2}\left\{\delta_{l_1l_2}\bar{l}'[(F_\gamma^L)_{l'l}\gamma_\mu P_L + (F_\gamma^R)_{l'l}\gamma_\mu P_R + \frac{(\not{p}-\not{p}')}{(p-p')^2}((G_\gamma^L)_{l'l}\gamma_\mu P_L + (G_\gamma^R)_{l'l}\gamma_\mu P_R)]l\bar{l}_1\gamma^\mu l_2^C - [l'\leftrightarrow l_1]\right\}, \quad (3.5)$$

$$\mathcal{T}_Z^{ll'l_1l_2} = \frac{\alpha_w^2}{2M_W^2}[\delta_{l_1l_2}\bar{l}'((F_Z^L)_{l'l}\gamma_\mu P_L + (F_Z^R)_{l'l}\gamma_\mu P_R)l\bar{l}_1(g_L^l\gamma^\mu P_L + g_R^l\gamma^\mu P_R)l_2^C - (l'\leftrightarrow l_1)], \quad (3.6)$$

$$\mathcal{T}_{\text{box}}^{ll'l_1l_2} = -\frac{\alpha_w^2}{4M_W^2}(B_{\ell V}^{LL}\bar{l}'\gamma_\mu P_L l\bar{l}_1\gamma^\mu P_L l_2^C + B_{\ell V}^{RR}\bar{l}'\gamma_\mu P_R l\bar{l}_1\gamma^\mu P_R l_2^C + B_{\ell V}^{LR}\bar{l}'\gamma_\mu P_L l\bar{l}_1\gamma^\mu P_R l_2^C + B_{\ell V}^{RL}\bar{l}'\gamma_\mu P_R l\bar{l}_1\gamma^\mu P_L l_2^C$$

$$+ B_{\ell S}^{LL}\bar{l}'P_L l\bar{l}_1 P_L l_2^C + B_{\ell S}^{RR}\bar{l}'P_R l\bar{l}_1 P_R l_2^C + B_{\ell S}^{LR}\bar{l}'P_L l\bar{l}_1 P_R l_2^C + B_{\ell S}^{RL}\bar{l}'P_R l\bar{l}_1 P_L l_2^C + B_{\ell T}^{LL}\bar{l}'\sigma_{\mu\nu}P_L l\bar{l}_1\sigma^{\mu\nu}P_L l_2^C$$

$$+ B_{\ell T}^{RR}\bar{l}'\sigma_{\mu\nu}P_R l\bar{l}_1\sigma^{\mu\nu}P_R l_2^C) \quad (3.7)$$

$$\equiv -\frac{\alpha_w^2}{4M_W^2}\sum_{X,Y=L,R}\sum_{A=V,S,T}B_{\ell A}^{XY}\bar{l}'\Gamma_A^X l\bar{l}_1\Gamma_A^Y l_2^C, \quad (3.8)$$

where $g_L^l = -1/2 + s_w^2$ and $g_R^l = s_w^2$ are Z-boson-lepton couplings and $s_w = \sin\theta_w$. The composite box form factors $B_{\ell A}^{XY}$, $A = V$, S, T, X, $Y = L$, R are given in Appendix C. The labels V, S and T denote the form factors of the vector, scalar and tensor combinations of the currents, while L and R distinguish between left and right chiralities of these currents. We note that the box form factors contain both direct and Fierz-transformed contributions. Equation (3.8) represents a shorthand expression that takes account of all individual contributions to the amplitude $\mathcal{T}_{\text{box}}^{ll'l_1l_2}$ induced by box graphs. Explicitly, the matrices Γ_A^X appearing in (3.8) read

$$(\Gamma_V^L, \Gamma_V^R, \Gamma_S^L, \Gamma_S^R, \Gamma_T^L, \Gamma_T^R)$$
$$= (\gamma_\mu P_L, \gamma_\mu P_R, P_L, P_R, \sigma_{\mu\nu}P_L, \sigma_{\mu\nu}P_R). \quad (3.9)$$

Notice that the tensor form factors $B_{\ell T}^{LR}$ and $B_{\ell T}^{RL}$ vanish in the sum (3.8), i.e. $B_{\ell T}^{LR} = B_{\ell T}^{RL} = 0$, as a consequence of the identity $\sigma^{\mu\nu}\gamma_5 = -\frac{i}{2}\varepsilon^{\mu\nu\rho\tau}\sigma_{\rho\tau}$. A very similar chiral structure holds also true for the semileptonic box amplitudes defined in the next section. We should remark here that [37,52] do not include in their calculations the chiral structures $P_L \times P_R$ and $P_R \times P_L$ and their corresponding form factors $B_{\ell S}^{LR}$ and $B_{\ell S}^{RL}$.

In a three-generation model, the transition amplitude for the decays $l \rightarrow l'l_1l_2^C$ may fall in one of the following three classes or categories [33]: (i) $l' \neq l_1 = l_2$, (ii) $l' = l_1 = l_2$, and (iii) $l' = l_1 \neq l_2$. In the first two classes (i) and (ii), the total lepton number is conserved, whilst in the third class (iii) the total lepton number is violated by two units. Here, we ignore this lepton-number violating class (iii) of charged lepton decays, since the predictions turn out to be unobservably small in the ν_RMSSM. Moreover, we suppress the universal indices $l'l$ that appear in the photon and Z-boson form factors, i.e. F_γ^L, F_γ^R, F_Z^L and F_Z^R. Given the above simplification and the notation of the box form factors in (3.8), the branching ratios for the class (i) and (ii) of CLFV three-body decays are given by

$$B(l \rightarrow l'l_1l_1^C) = \frac{m_l^5\alpha_w^4}{24576\pi^3 M_W^4\Gamma_l}\left\{[|2s_w^2(F_\gamma^L + F_Z^L) - F_Z^L - B_{\ell V}^{LL}|^2 + |2s_w^2(F_\gamma^R + F_Z^R) - B_{\ell V}^{RR}|^2 + |2s_w^2(F_\gamma^L + F_Z^L)\right.$$

$$- B_{\ell V}^{LR}|^2 + |2s_w^2(F_\gamma^R + F_Z^R) - F_Z^R - B_{\ell V}^{RL}|^2] + \frac{1}{4}(|B_{\ell S}^{LL}|^2 + |B_{\ell S}^{RR}|^2 + |B_{\ell S}^{LR}|^2 + |B_{\ell S}^{RL}|^2)$$

$$+ 12(|B_{\ell T}^{LL}|^2 + |B_{\ell T}^{RR}|^2) + \frac{32s_w^4}{m_l}[\text{Re}((F_\gamma^R + F_Z^R)G_\gamma^{L*}) + \text{Re}((F_\gamma^L + F_Z^L)G_\gamma^{R*})]$$

$$- \frac{8s_w^2}{m_l}[\text{Re}((F_Z^R + B_{\ell V}^{RR} + B_{\ell V}^{RL})G_\gamma^{L*}) + \text{Re}((F_Z^L + B_{\ell V}^{LL} + B_{\ell V}^{LR})G_\gamma^{R*})]$$

$$+ \frac{32s_w^4}{m_l^2}(|G_\gamma^L|^2 + |G_\gamma^R|^2)\left(\ln\frac{m_l^2}{m_{l'}^2} - 3\right)\right\}, \quad (3.10)$$

$$B(l \to l'l'l'^C) = \frac{m_l^5 \alpha_w^4}{24576\pi^3 M_W^4 \Gamma_l} \left\{ 2 \left[\left| 2s_w^2(F_\gamma^L + F_Z^L) - F_Z^L - \frac{1}{2}B_{\ell V}^{LL} \right|^2 + \left| 2s_w^2(F_\gamma^R + F_Z^R) - \frac{1}{2}B_{\ell V}^{RR} \right|^2 \right] \right.$$

$$+ |2s_w^2(F_\gamma^L + F_Z^L) - B_{\ell V}^{LR}|^2 + |2s_w^2(F_\gamma^R + F_Z^R) - (F_Z^R + B_{\ell V}^{RL})|^2 + \frac{1}{8}(|B_{\ell S}^{LL}|^2 + |B_{\ell S}^{RR}|^2)$$

$$+ 6(|B_{\ell T}^{LL}|^2 + |B_{\ell T}^{RR}|^2) + \frac{48s_w^4}{m_l}[\text{Re}((F_\gamma^R + F_Z^R)G_\gamma^{L*}) + \text{Re}((F_\gamma^L + F_Z^L)G_\gamma^{R*})]$$

$$- \frac{8s_w^2}{m_l}[\text{Re}((F_Z^R + B_{\ell V}^{RR} + B_{\ell V}^{RL})G_\gamma^{L*}) + \text{Re}((2F_Z^L + B_{\ell V}^{LL} + B_{\ell V}^{LR})G_\gamma^{R*})]$$

$$+ \frac{32s_w^4}{m_l^2}(|G_\gamma^L|^2 + |G_\gamma^R|^2)\left(\ln\frac{m_l^2}{m_{l'}^2} - \frac{11}{4} \right) \right\}, \tag{3.11}$$

where m_l and $m_{l'}$, m_{l_1}, m_{l_2} are the masses of the initial- and final-state charged leptons and Γ_l is the decay width of the charged lepton l. Here we should emphasize that the transition amplitudes (3.5), (3.6), and (3.7) and the branching ratios (3.10) and (3.11) have the most general chiral and form factor structure to leading order in external masses and momenta and so they are applicable to most models of new physics with CLFV. Finally, we have checked that the branching ratios (3.10) and (3.11) go over to the results of Ref. [33], in the ν_RSM limit of the theory.

C. Coherent $\mu \to e$ conversion in a nucleus

The coherent $\mu \to e$ conversion in a nucleus corresponds to the process $J_\mu \to e^- J^+$, where J_μ is an atom of nucleus J with one orbital electron replaced by a muon and J^+ is the corresponding ion without the muon. The transition amplitude for such a CLFV process,

$$\mathcal{T}^{\mu e;J} = \langle J^+ e^- | \mathcal{T}^{d\mu \to de} | J_\mu \rangle + \langle J^+ e^- | \mathcal{T}^{u\mu \to ue} | J_\mu \rangle, \tag{3.12}$$

depends on two effective box operators,

$$\mathcal{T}_{\text{box}}^{d\mu \to de} = -\frac{\alpha_w^2}{4M_W^2} \sum_{X,Y=L,R} \sum_{A=V,S,T} B_{dA}^{XY} \bar{e}\Gamma_A^X \mu \bar{d}\Gamma_A^X d$$

$$= -\frac{\alpha_w^2}{2M_W^2}(d^\dagger d)\bar{e}(V_d^R P_R + V_d^L P_L)\mu, \tag{3.13}$$

$$\mathcal{T}_{\text{box}}^{u\mu \to ue} = -\frac{\alpha_w^2}{4M_W^2} \sum_{X,Y=L,R} \sum_{A=V,S,T} B_{uA}^{XY} \bar{e}\Gamma_A^X \mu \bar{u}\Gamma_A^X u$$

$$= -\frac{\alpha_w^2}{2M_W^2}(u^\dagger u)\bar{e}(V_u^R P_R + V_u^L P_L)\mu. \tag{3.14}$$

Here μ and e are the muon and electron wave functions and d and u are field operators acting on the J_μ and J^+ states. The form factors B_{dA}^{XY} and B_{uA}^{XY} are given in Appendix C. The composite form factors V_d^L, V_u^L, V_d^R, V_u^R may conveniently be expressed as

$$V_d^L = -\frac{1}{3}s_w^2\left(F_\gamma^L - \frac{1}{m_\mu}G_\gamma^R \right) + \left(\frac{1}{4} - \frac{1}{3}s_w^2 \right)F_Z^L$$

$$+ \frac{1}{4}(B_{dV}^{LL} + B_{dV}^{LR} + B_{dS}^{RR} + B_{dS}^{RL}),$$

$$V_d^R = -\frac{1}{3}s_w^2\left(F_\gamma^R - \frac{1}{m_\mu}G_\gamma^L \right) + \left(\frac{1}{4} - \frac{1}{3}s_w^2 \right)F_Z^R$$

$$+ \frac{1}{4}(B_{dV}^{RR} + B_{dV}^{RL} + B_{dS}^{LL} + B_{dS}^{LR}),$$

$$V_u^L = \frac{2}{3}s_w^2\left(F_\gamma^L - \frac{1}{m_\mu}G_\gamma^R \right) + \left(-\frac{1}{4} + \frac{2}{3}s_w^2 \right)F_Z^L$$

$$+ \frac{1}{4}(B_{uV}^{LL} + B_{uV}^{LR} + B_{uS}^{RR} + B_{uS}^{RL}),$$

$$V_u^R = \frac{2}{3}s_w^2\left(F_\gamma^R - \frac{1}{m_\mu}G_\gamma^L \right) + \left(-\frac{1}{4} + \frac{2}{3}s_w^2 \right)F_Z^R$$

$$+ \frac{1}{4}(B_{uV}^{RR} + B_{uV}^{RL} + B_{uS}^{LL} + B_{uS}^{LR}), \tag{3.15}$$

where $F_\gamma^L, F_\gamma^R, F_Z^L, F_Z^R$ is the shorthand notation for $(F_\gamma^L)_{e\mu}$, $(F_\gamma^R)_{e\mu}, (F_Z^L)_{e\mu}, (F_Z^R)_{e\mu}$.

Our next step is to determine the nucleon matrix elements of the operators $u^\dagger u$ and $d^\dagger d$. These are given by

$$\langle J^+ e^- | u^\dagger u | J_\mu \rangle = (2Z + N)F(-m_\mu^2),$$
$$\langle J^+ e^- | d^\dagger d | J_\mu \rangle = (Z + 2N)F(-m_\mu^2), \tag{3.16}$$

where the form factor $F(q^2)$ incorporates the recoil of the J^+ ion [53], and the factors $2Z + N$ and $Z + 2N$ count the number of u and d quarks in the nucleus J, respectively. Hence, the matrix element for $J_\mu \to J^+ \mu^-$ can be written down as

$$T^{J_\mu \to J^+ e^-} = -\frac{\alpha_w^2}{2M_W^2}F(-m_\mu^2)\bar{e}(Q_W^L P_R + Q_W^R P_L)\mu, \tag{3.17}$$

with

$$Q_W^L = (2Z + N)V_u^L + (Z + 2N)V_d^L,$$
$$Q_W^R = (2Z + N)V_u^R + (Z + 2N)V_d^R. \tag{3.18}$$

Given the transition amplitude (3.17), the decay rate $J_\mu \to J^+ e^-$ is found to be

$$R_{\mu e}^J = \frac{\alpha^3 \alpha_w^4 m_\mu^5}{16\pi^2 M_W^4 \Gamma_{\text{capture}}} \frac{Z_{\text{eff}}^4}{Z} |F(-m_\mu^2)|^2 (|Q_W^L|^2 + |Q_W^R|^2),$$

(3.19)

where Γ_{capture} is the capture rate of the muon by the nucleus, and Z_{eff} is the effective charge which takes into account coherent effects that can occur in the nucleus J due to its finite size. In our analysis, we use the values of Z_{eff} quoted in Ref. [54]. We reiterate that the branching ratio (3.19) possesses the most general form factor structure to leading order in external masses and momenta and is relevant to most models of new physics with CLFV. Finally, we have verified that our analytical results are consistent with Refs. [34,55,56] in the ν_RSM limit of the theory.

IV. NUMERICAL RESULTS

In this section, we present a numerical analysis of CLFV observables in the ν_RMSSM. In order to reduce the number of independent parameters, we adopt the constrained framework of mSUGRA. In detail, our model parameters are (i) the usual SM parameters, such as gauge-coupling constants, the quark and charged lepton Yukawa matrices inputted at the scale M_Z, (ii) the heavy neutrino mass m_N and the neutrino Yukawa matrix $\mathbf{h}_\nu$ evaluated at m_N, (iii) the universal mSUGRA parameters m_0, $M_{1/2}$ and A_0 inputted at the GUT scale, and (iv) the ratio $\tan\beta$ of the Higgs VEVs and the sign of the superpotential Higgs-mixing parameter μ.

The allowed ranges of the soft SUSY-breaking parameters m_0, $M_{1/2}$, A_0 and $\tan\beta$ are strongly constrained by a number of accelerator and cosmological data [21,22,46,57]. For definiteness, we consider the following set of input parameters:

$$\tan\beta = 10, \qquad m_0 = 1000 \text{ GeV},$$
$$A_0 = -3000 \text{ GeV}, \qquad M_{1/2} = 1000 \text{ GeV}.$$

(4.1)

Here we take the μ parameter to be positive, whilst its absolute value $|\mu|$ is derived form the minimization of the Higgs potential at the scale M_Z. With aid of Refs. [58–60], we verify that the parameter set (4.1) predicts a SM-like Higgs boson with $m_H \approx 125$ GeV, in agreement with the recent discovery at the LHC [21,22], and is compatible with the current lower limits on gluino and squark masses [46]. The set (4.1) is also in agreement with having the lightest neutralino as the Dark Matter in the Universe [57].

We employ the one-loop RG equations of Refs. [61,62] to evolve the the gauge-coupling constants and the quark and charged lepton Yukawa matrices from M_Z to the GUT scale, while the heavy neutrino mass matrix $\mathbf{m}_M$ and the neutrino Yukawa matrix $\mathbf{h}_\nu$ are evolved from the heavy neutrino mass threshold m_N to the GUT scale. Furthermore, we assume that the heavy neutrino-sneutrino sector is supersymmetric above m_N. For purposes of RG

evolution, this is a good approximation for m_N larger than the typical soft SUSY-breaking scale [34]. At the GUT scale, the mSUGRA universality conditions are used to express the soft SUSY-breaking masses, in terms of m_0, $M_{1/2}$ and A_0. Hence, all scalar masses receive a soft SUSY-breaking mass m_0, all gaugino are mass degenerate to $M_{1/2}$, and all scalar trilinear couplings are of the form $\mathbf{h}_x A_0$, with $x = u$, d, l, ν, where $\mathbf{h}_x$ are the Yukawa matrices at the GUT scale. The sneutrino mass matrix acquires additional contributions from the heavy neutrino mass matrix. The sparticle mass matrices and trilinear couplings are evolved from the GUT scale to M_Z, except for the sneutrino masses which are evolved to the heavy neutrino threshold m_N. Having thus obtained all sparticle and sneutrino mass matrices, we can numerically evaluate all particle masses and interaction vertices in the ν_RMSSM, without approximations.

To simplify our numerical analysis, we consider two representative scenarios of Yukawa textures discussed in Sec. II. Specifically, the first scenario realizes the U(1)-symmetric Yukawa texture in (2.4), for which we take either $a = b$ and $c = 0$, or $a = c$ and $b = 0$, or $b = c$ and $a = 0$, thus giving rise to CLFV processes $\mu \to eX$, $\tau \to eX$ and $\tau \to \mu X$, respectively. Here X represents the lepton flavor conserving state(s), e.g. $X = \gamma$, e^+e^-, $\mu^+\mu^-$, $q\bar{q}$. The second scenario is motivated by the A_4 group and uses the Yukawa texture (2.5), where the parameters a, b and c are taken to be all equal, i.e. $a = b = c$.

The heavy neutrino mass scale m_N strongly depends on the size of the symmetry-breaking terms in the Yukawa matrix $\mathbf{h}_\nu$. For instance, for the model (2.4), the typical values of the U(1)-lepton-symmetry-breaking parameters $\epsilon_l \equiv \epsilon_{e,\mu,\tau}$ consistent with low-scale resonant leptogenesis is $\epsilon \lesssim 10^{-5}$ [30], leading to light-neutrino masses

$$m_\nu \sim \frac{\epsilon_l^2 v^2}{m_N} \sim 10^{-2} \text{ eV} \left(\frac{\epsilon_l}{10^{-6}}\right)^2 \left(\frac{1 \text{ TeV}}{m_N}\right).$$

(4.2)

Taking into account the constraint $m_\nu \gtrsim 10^{-1}$ eV generically derived from neutrino oscillation data, we may estimate that the heavy neutrino mass scale m_N is typically restricted to be less than 10 TeV, for $\epsilon_l = 10^{-5}$. If the assumption of successful low-scale leptogenesis is relaxed, the symmetry-breaking parameters ϵ_l has only to be couple of orders in magnitude smaller than the Yukawa parameters a, b and c, with a, b, $c \lesssim 10$. Thus, for $\epsilon_l < 10^{-3} - 10^{-2}$, the heavy neutrino mass scale m_N may be as large as $10^7 - 10^9$ TeV, leading to the decoupling of heavy neutrinos from low-energy observables. As our interest is in the interplay between heavy neutrino, sneutrino and soft SUSY-breaking contributions to CLFV observables, we will only study here the parameter space in which $m_N < 10$ TeV.

In the present analysis, we consider that the symmetry-preserving Yukawa parameters a, b and c are limited
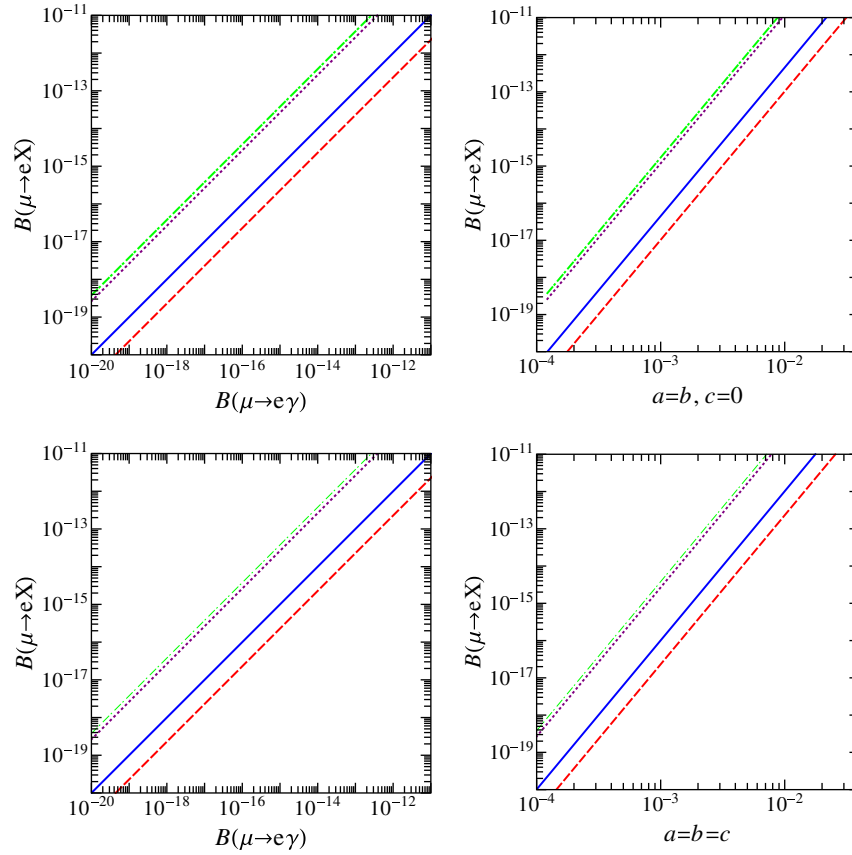
FIG. 3 (color online). Numerical estimates of $B(\mu \to e\gamma)$ [blue (solid)], $B(\mu \to eee)$ [red (dashed)], $R_{\mu e}^{\mathrm{Ti}}$ [violet (dotted)] and $R_{\mu e}^{\mathrm{Au}}$ [green (dash-dotted)], as functions of $B(\mu \to e\gamma)$ (left panels) and the Yukawa parameter a (right panels), for $m_N = 400$ GeV and $\tan \beta = 10$. The upper two panels correspond to the Yukawa texture (2.4), with $a = b$ and $c = 0$, and the lower two panels to the Yukawa texture (2.5), with $a = b = c$.

through the perturbativity condition: $\mathrm{Tr}\,\mathbf{h}_\nu^\dagger \mathbf{h}_\nu < 4\pi$, which we require to hold true for the entire interval of the RG evolution: $\ln(M_Z/\mathrm{TeV}) < t < \ln(M_{\mathrm{GUT}}/\mathrm{TeV})$. For the model in (2.4), this condition translates into the constraint: $a < 0.34$, and for the model in (2.5), to $a < 0.23$. As a consequence, we do not display in plots numerical values for points in parameter space, for which the aforementioned perturbativity condition gets violated.

In Fig. 3, we display numerical predictions for the μ-LFV observables $B(\mu \to eX)$: $B(\mu \to e\gamma)$ [blue (solid) line], $B(\mu \to eee)$ [red (dashed) line], $R_{\mu e}^{\mathrm{Ti}}$ [violet (dotted) line] and $R_{\mu e}^{\mathrm{Au}}$ [green (dash-dotted) line], as functions of $B(\mu \to e\gamma)$ (left panels) and the Yukawa parameter a (right panels), for $m_N = 400$ GeV and $\tan \beta = 10$. The upper two panels assume the Yukawa texture in (2.4), with $a = b$ and $c = 0$, whilst the lower two panels correspond to the Yukawa texture in (2.5), with $a = b = c$. In Fig. 4, we give numerical estimates for the same set of μ-LFV observables, but for $m_N = 1$ TeV. In Figs. 3 and 4, the Yukawa parameter a has been chosen, such that $10^{-20} < B(\mu \to e\gamma) < 10^{-10}$. Such a range of values includes both the present [7–10,63,64] and future [16,17,19,65–68] experimental limits. As we see from

Figs. 3 and 4, the CLFV observables under study depend quadratically on the Yukawa parameter a, namely they are proportional to a^2. Instead, the quartic Yukawa terms proportional to a^4 [34] remain always small, which is a consequence of the imposed perturbativity constraint: $\mathrm{Tr}(\mathbf{h}_\nu^\dagger \mathbf{h}_\nu) < 4\pi$, up to the GUT scale.

By analogy, Figs. 5 and 6 present numerical estimates of the τ-LFV observables $B(\tau \to eX)$: $B(\tau \to e\gamma)$ [blue (solid) lines], $B(\tau \to eee)$ [red (dashed) lines] and $B(\tau \to e\mu\mu)$ [violet (dotted) lines], as functions of $B(\tau \to e\gamma)$ (left panels) and the Yukawa parameter a (right panels), for $m_N = 400$ GeV and $m_N = 1$ TeV, respectively. Note that we do not show predictions for the fully complementary observables $B(\tau \to \mu X)$: $B(\tau \to \mu\gamma)$, $B(\tau \to \mu\mu\mu)$ and $B(\tau \to \mu ee)$. The upper panels give our predictions for the Yukawa texture (2.4), with $a = c$ and $b = 0$, and the lower panels for the Yukawa texture (2.5), with $a = b = c$. In both Figs. 5 and 6, the Yukawa parameter a has been chosen, such that $10^{-16} < B(\tau \to e\gamma) < 10^{-7}$. As can be seen from Figs. 5 and 6, all observables $B(\tau \to eX)$ of τ-LFV (with $X = \gamma$, ee, $\mu\mu$) exhibit similar quadratic dependence on the small Yukawa parameter a. However, close to the largest perturbatively allowed values of a, i.e.
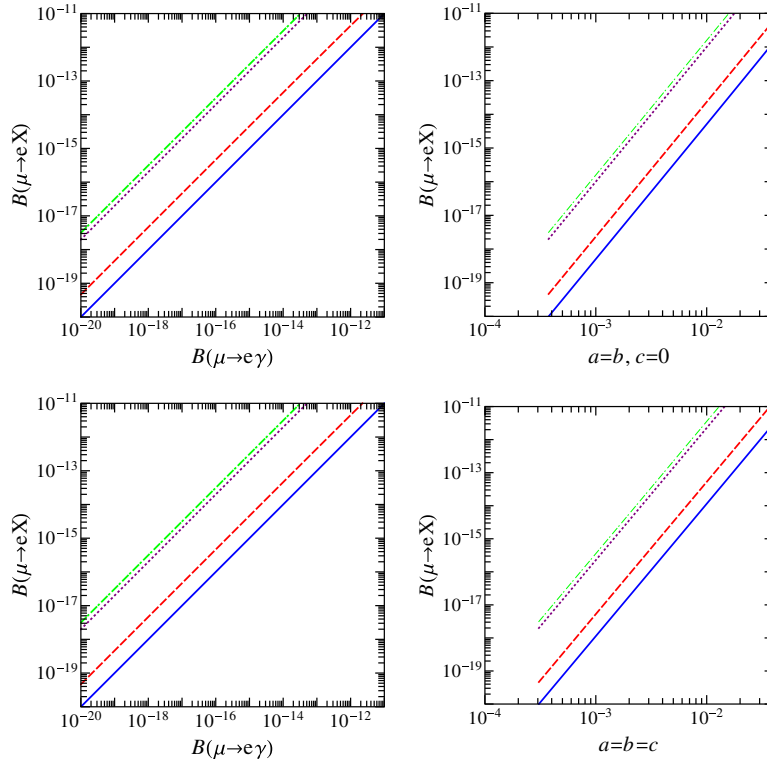
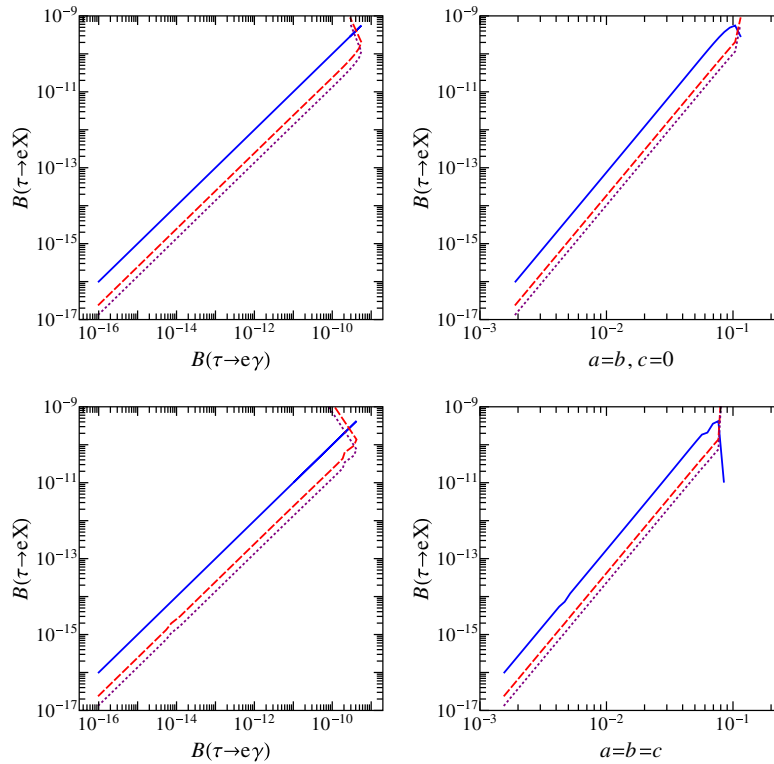FIG. 4 (color online).   The same as in Fig. 3, but for $m_N = 1$ TeV.

FIG. 5 (color online).   Numerical estimates of $B(\tau \to e\gamma)$ [blue (solid)], $B(\tau \to eee)$ [red (dashed)] and $B(\tau \to e\mu\mu)$ [violet (dotted)], as functions of $B(\tau \to e\gamma)$ (left panels) and the Yukawa parameter a (right panels), for $m_N = 400$ GeV and $\tan \beta = 10$. The upper panels present predictions for the Yukawa texture (2.4), with $a = c$ and $b = 0$, and the lower panels for the Yukawa texture (2.5), with $a = b = c$.
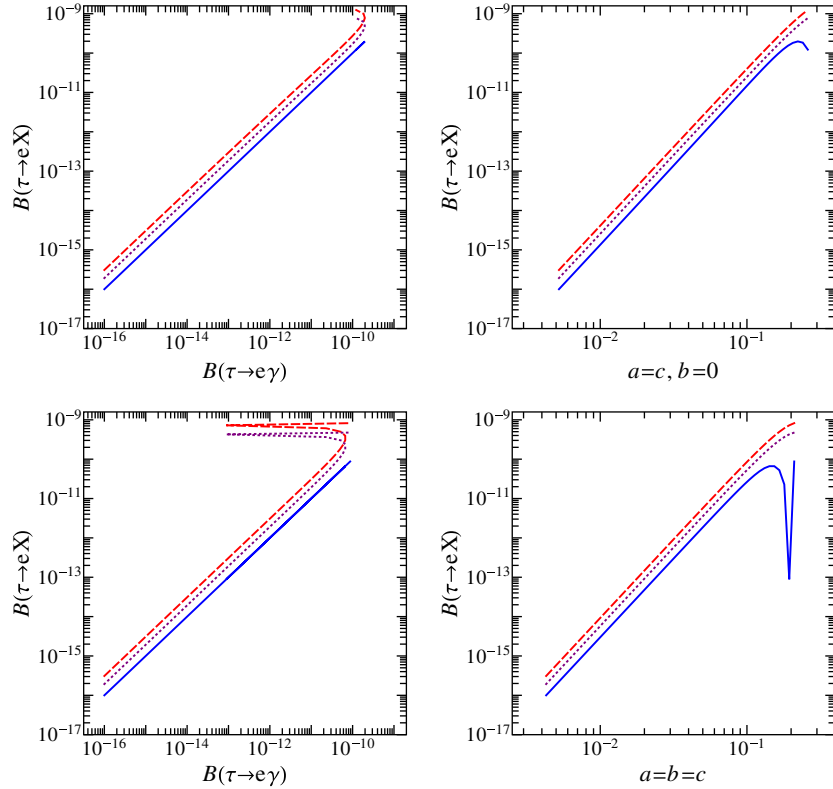
FIG. 6 (color online). The same as in Fig. 5, but for $m_N = 1$ TeV.

$a \lesssim 0.34$ for the model (2.4) and $a \lesssim 0.23$ for the model (2.5), some of the observables of τ-LFV exhibit either numerical instability, or the existence of a cancellation region in parameter space, as we will see below.

Figure 7 presents numerical estimates of $B(\mu \to e\gamma)$ [blue (solid) line], $B(\mu \to eee)$ [red (dashed) line], $R_{\mu e}^{\mathrm{Ti}}$ [violet (dotted) line] and $R_{\mu e}^{\mathrm{Au}}$ [green (dash-dotted) line], as functions of $B(\mu \to e\gamma)$ (left panels) and the heavy neutrino mass scale m_N (right panels). In all panels, we keep the Yukawa parameter a fixed by the condition $B(\mu \to e\gamma) = 10^{-12}$ for $m_N = 400$ GeV, using the benchmark value: $\tan\beta = 10$. The upper panels display numerical values for the Yukawa texture (2.4), with $a = b$ and $c = 0$, and the lower panels for the Yukawa texture (2.5), with $a = b = c$. The heavy neutrino mass is varied within the LHC explorable range: 400 GeV $< m_N <$ 10 TeV. All observables $B(\mu \to eX)$ of μ-LFV (with $X = \gamma$, ee, Ti, Au) exhibit a nontrivial dependence on m_N. The branching ratio $B(\mu \to e\gamma)$ shows a dip at $m_N \approx 800$ GeV in both models (2.4) and (2.5), signifying the existence of a cancellation region in parameter space, due to loops involving heavy neutrino, sneutrino and soft SUSY-breaking terms. For $m_N \gtrsim 3$ TeV, all observables tend to a constant value, as a result of the dominance of the soft SUSY-breaking contributions.

In Fig. 8 we show contours of the Yukawa parameters (a, b, c) versus the heavy neutrino mass scale m_N, for $B(\mu \to e\gamma)$ [blue (solid) line], $B(\mu \to eee)$ [red (dashed) line], $R_{\mu e}^{\mathrm{Ti}}$ [violet (dotted) line] and $R_{\mu e}^{\mathrm{Au}}$ [green (dash-dotted) line]. The Yukawa parameters a and m_N are determined by the condition $B(\mu \to e\gamma) = 10^{-12}$. The labels in the vertical axes indicate the two Yukawa textures in (2.4) and (2.5), which we have adopted in our analysis. The contours for $B(\mu \to e\gamma)$ display a maximum for $m_N \approx$ 800 GeV, as a consequence of cancellations between heavy neutrino, sneutrino and soft SUSY-breaking contributions (cf. Fig. 7).

Figure 9 shows contours of the Yukawa parameters (a, b, c), as functions of m_N, for $B(\tau \to e\gamma)$ [blue (solid) line], where the parameters a and m_N are determined by the condition $B(\tau \to e\gamma) = 10^{-9}$. We do not give numerical results for $B(\tau \to \mu\gamma)$, as these are fully complementary to the ones given for $B(\tau \to e\gamma)$. Notice that given the above condition on $B(\tau \to e\gamma)$, no solution exists for $B(\tau \to eee)$ and $B(\tau \to e\mu\mu)$.

In our numerical analysis so far, we have kept the value of $\tan\beta$ fixed to its benchmark value given in (4.1): $\tan\beta = 10$. In Fig. 10, we relax this assumption, varying $\tan\beta$ in the interval $5 \lesssim \tan\beta \lesssim 20$, while maintaining agreement with a SM-like Higgs-boson mass $M_H \approx$ 125 GeV and taking into account that the combined experimental and theoretical errors are currently of the order of 5–6 GeV. Specifically, in Fig. 10 we display the dependence of $B(\mu \to e\gamma)$ [blue (solid) line], $B(\mu \to eee)$ [red (dashed) line], $R_{\mu e}^{\mathrm{Ti}}$ [violet (dotted) line] and $R_{\mu e}^{\mathrm{Au}}$ [green (dash-dotted; not observable in black-and-white printout)
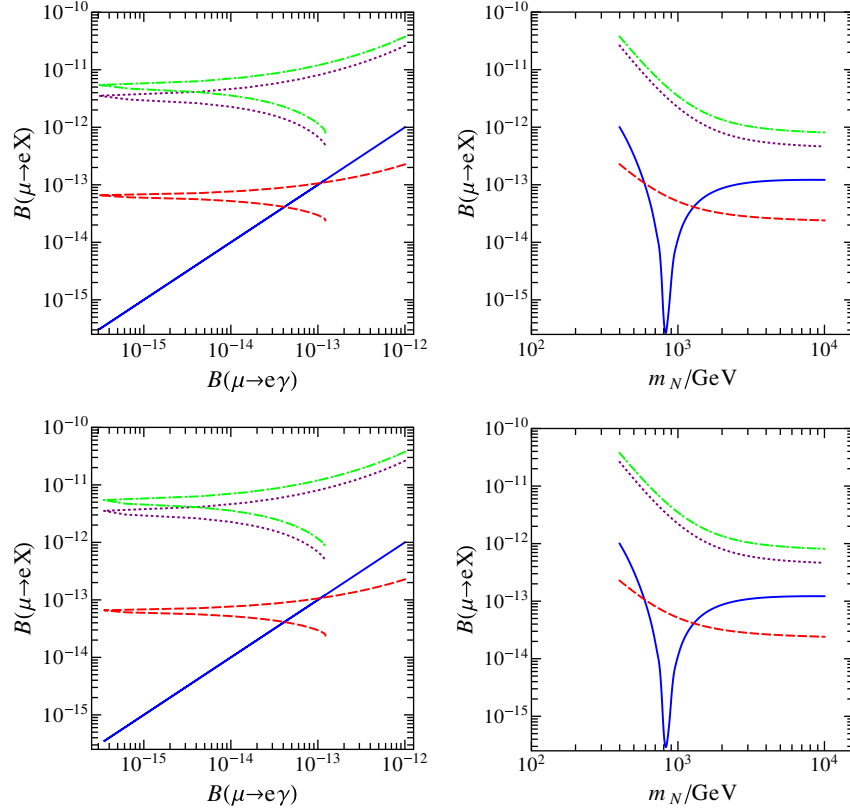
FIG. 7 (color online).   Numerical estimates of $B(\mu \to e\gamma)$ [blue (solid)], $B(\mu \to eee)$ [red (dashed)], $R_{\mu e}^{\text{Ti}}$ [violet (dotted)] and $R_{\mu e}^{\text{Au}}$ [green (dash-dotted)], as functions of $B(\mu \to e\gamma)$ (left panels) and the heavy neutrino mass scale m_N (right panels). In all panels, the Yukawa parameter a was kept fixed by the condition $B(\mu \to e\gamma) = 10^{-12}$ for $m_N = 400$ GeV, and $\tan\beta = 10$ was used. The upper panels display numerical values for the Yukawa texture (2.4), with $a = b$ and $c = 0$, and the lower panels for the Yukawa texture (2.5), with $a = b = c$.

line] on $\tan\beta$. In all panels, the Yukawa parameter a is determined by the condition $B(\mu \to e\gamma) = 10^{-12}$. The upper panels in Fig. 10 show numerical results for $m_N = 400$ GeV, while the lower panels for $m_N = 1$ TeV. The left panels give our predictions for the Yukawa texture (2.4), with $a = b$ and $c = 0$, and the right panels for the Yukawa texture (2.5), with $a = b = c$. In the lower panels, we observe a suppression of $B(\mu \to e\gamma)$, for values

$\tan\beta \approx 7$, due to cancellation between heavy neutrino, sneutrino and soft SUSY-breaking effects.

It is interesting to compare the contributions of the magnetic dipole form factors to the CLFV observables, with those originating from the remaining form factors. Specifically, if one assumes that only the magnetic dipole form factors $G_\gamma^{L,R}$ contribute in (3.10), (3.11), and (3.19), then the following analytical results are obtained for the ratios:
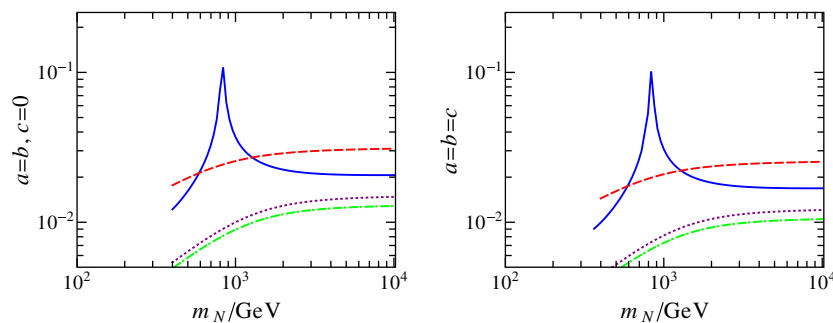

FIG. 8 (color online).   Contours of the Yukawa parameters (a, b, c) versus m_N, for $B(\mu \to e\gamma)$ [blue (solid)], $B(\mu \to eee)$ [red (dashed)], $R_{\mu e}^{\text{Ti}}$ [violet (dotted)] and $R_{\mu e}^{\text{Au}}$ [green (dash-dotted)], where a and m_N are determined by the condition $B(\mu \to e\gamma) = 10^{-12}$. All contours are evaluated with $\tan\beta = 10$ and for different Yukawa textures, as indicated by the vertical axes labels.
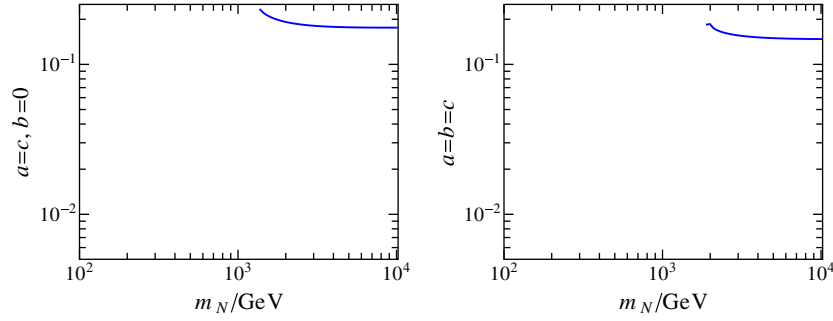
FIG. 9 (color online).   Contours of the Yukawa parameters (a, b, c) versus m_N, for $B(\tau \to e\gamma)$ [blue (solid)], where $\tan\beta = 10$ and a and m_N are determined by the condition $B(\tau \to e\gamma) = 10^{-9}$. No solutions have been found for $B(\tau \to eee)$ and $B(\tau \to e\mu\mu)$.

$$R_1 \equiv \frac{B(l \to l' l_1 l_1^c)}{B(l \to l'\gamma)} = \frac{\alpha}{3\pi}\left(\ln\frac{m_l^2}{m_{l'}^2} - 3\right), \qquad (4.3)$$

$$R_2 \equiv \frac{B(l \to l' l' l'^c)}{B(l \to l'\gamma)} = \frac{\alpha}{3\pi}\left(\ln\frac{m_l^2}{m_{l'}^2} - \frac{11}{4}\right), \qquad (4.4)$$

$$R_3 \equiv \frac{R_{\mu e}^J}{B(\mu \to e\gamma)} = 16\alpha^4 \frac{\Gamma_\mu}{\Gamma_{\text{capture}}} ZZ_{\text{eff}}^4|F(-\mu^2)|^2. \quad (4.5)$$

According to the formulas (4.3), (4.4), and (4.5), the predicted R_1 values for $\tau \to e\mu\mu$ and $\tau \to \mu ee$ are $1/90$ and $1/419$

respectively, the predicted R_2 values for $\mu \to eee$, $\tau \to eee$ and the $\tau \to \mu\mu\mu$ are $1/159$, $1/91$ and $1/460$ respectively, and the predicted R_3 values for Ti and Au are $1/198$ and $1/188$ respectively.

In Fig. 11, we give numerical estimates of the ratios $R_2(\mu \to eee)$, R_3^{Ti} and R_3^{Au}, as functions of m_N. The Yukawa parameter a is fixed by the condition $B(\mu \to e\gamma) = 10^{-12}$, for $m_N = 400$ GeV and $\tan\beta = 10$. In the upper panel, thick lines show the predicted values obtained by a complete evaluation of $R_2(\mu \to eee)$ [blue (solid) line], R_3^{Ti} [red (dashed) line] and R_3^{Au} [violet (dotted) line], while the respective thin lines are obtained by keeping only the
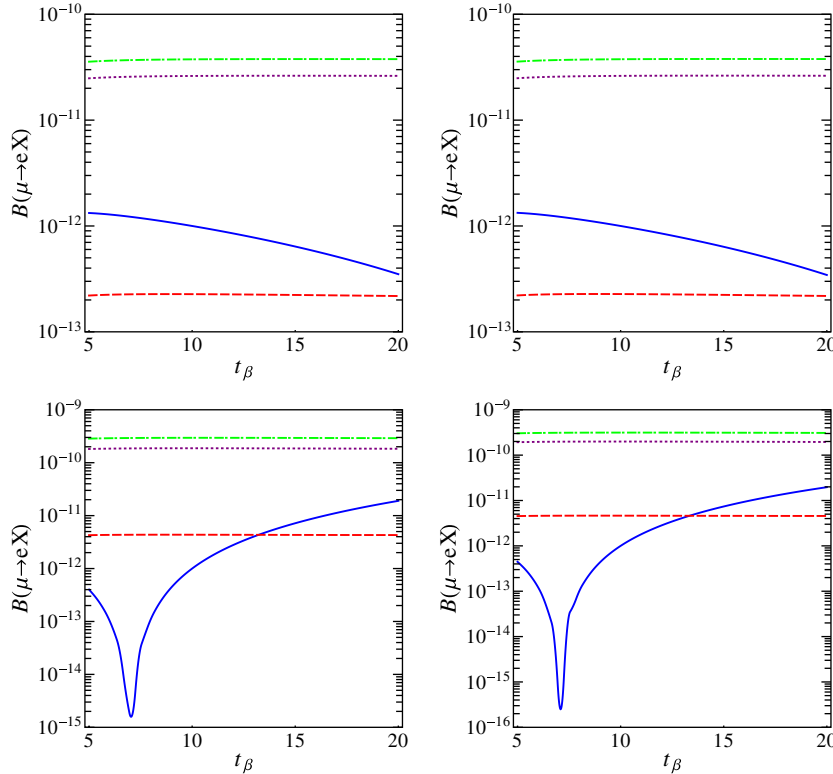

FIG. 10 (color online).   Numerical estimates of $B(\mu \to e\gamma)$ [blue (solid)], $B(\mu \to eee)$ [red (dashed)], $R_{\mu e}^{\text{Ti}}$ [violet (dotted)] and $R_{\mu e}^{\text{Au}}$ [green (dash-dotted)], as functions of $\tan\beta$. The upper panels are obtained for $m_N = 400$ GeV and the lower panels for $m_N = 1$ TeV. The left panels use the Yukawa texture (2.4), with $a = b$ and $c = 0$, and the right panels the Yukawa texture (2.5), with $a = b = c$. In all panels, the Yukawa parameter a is determined by the condition $B(\mu \to e\gamma) = 10^{-12}$.

magnetic dipole form factors G_γ^L and G_γ^R. Hence, we see that going beyond the magnetic dipole moment approximation may enhance the ratios $R_{2,3}$ by more than two orders of magnitude.

The two middle panels of Fig. 11 provide a form factor analysis of $R_2(\mu \to eee)$ and R_3^{Au}, by considering separately the contributions due to G_γ and F_γ [blue (solid) line], F_Z [red (dashed) line] and box form factors [violet (dotted) line]. In particular, we observe that heavy neutrino contributions to the box form factors become comparable to and even larger than the Z-boson-mediated graphs in $\mu \to e$ conversion in gold, for heavy neutrino masses $m_N \lesssim 1$ TeV. We have checked that for $m_N \lesssim 1$ TeV, box graphs due to heavy neutrinos also dominate the process of $\mu \to e$ conversion in titanium (not explicitly shown in Fig. 11). Finally, the two lower panels show
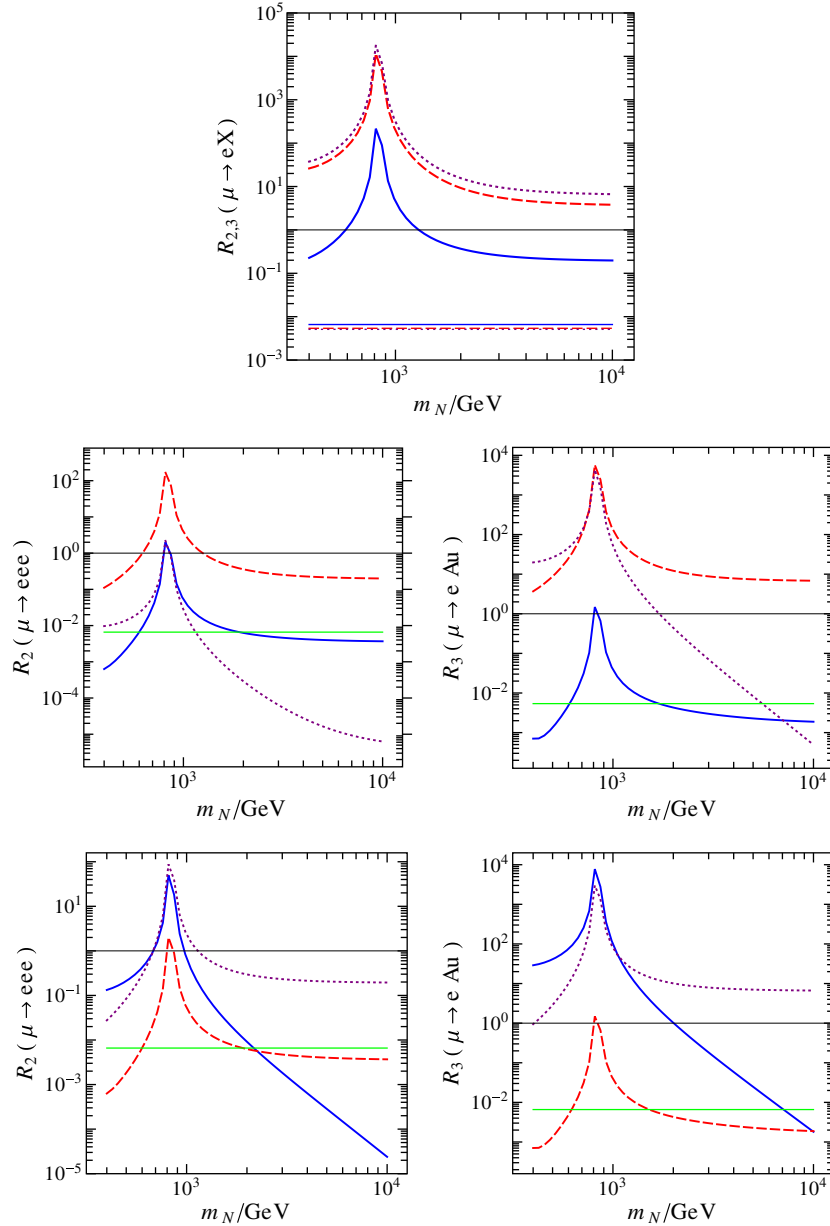

FIG. 11 (color online).   Numerical estimates of the ratios $R_2(\mu \to eee)$, R_3^{Ti} and R_3^{Au}, as functions of m_N. The Yukawa parameter a is fixed by the condition $B(\mu \to e\gamma) = 10^{-12}$, for $m_N = 400$ GeV and $\tan\beta = 10$. In the upper panel, thick lines give the complete evaluation of $R_2(\mu \to eee)$ [blue (solid)], R_3^{Ti} [red (dashed)] and R_3^{Au} [violet (dotted)], while the respective thin lines are evaluated keeping only the magnetic dipole form factors G_γ^L and G_γ^R. The two middle panels provide a form factor analysis of $R_2(\mu \to eee)$ and R_3^{Au}, in terms of contributions due to G_γ and F_γ [blue (solid)], F_Z [red (dashed)] and box form factors [violet (dotted)]. The lower two panels show the separate contributions due to heavy neutrinos N [blue (solid)], sneutrinos $\tilde{N}$ [red (dashed)] and soft SUSY-breaking LFV terms [violet (dotted)]. The green (horizontal) lines in the middle and lower panels give the predicted values obtained by assuming that only the $G_\gamma^{L,R}$ form factors contribute to the amplitudes.

the individual contributions due to heavy neutrinos $N_{1,2,3}$ [blue (solid) line], sneutrinos $\tilde{N}_{1,2,...,12}$ [red (dashed) line] and soft SUSY-breaking LFV terms [violet (dotted) line]. From these two lower panels, it is obvious that for heavy neutrino masses $m_N \lesssim 1$ TeV, the soft SUSY-breaking effects dominate the CLFV form factors, which are tagged with the superscripts SB in Appendix C. Instead, for $m_N \lesssim 1$ TeV, heavy neutrino effects start becoming the leading contribution to the CLFV observables associated with the muon. Note that the green (horizontal; not observable in black-and-out printout) lines in the middle and lower panels serve as reference values obtained by assuming that only the $G_\gamma^{L,R}$ form factors contribute to the amplitudes.

An important consistency check for our numerical analysis has been to *analytically* show that all soft SUSY-breaking effects on the form factors (C4), (C8), and (C14), vanish in the limit of degenerate charged slepton masses. On the other hand, RG effects from M_{GUT} to M_Z induce sizeable deviations to the charged slepton mass matrix from the unit matrix. As a consequence, unitarity cancellations due to the so-called Glashow-Iliopoulos-Maiani mechanism become less effective in this case and so render the SB part of the form factors, such as $F_{l'lZ}^{L,\mathrm{SB}}$ and $F_{l'lZ}^{R,\mathrm{SB}}$, rather large.

Another essential check was to show that under the assumptions adopted in Ref. [44], our form factor $F_{l'lZ}^{L,\tilde{N}}$ given in (C7) reduces to $\frac{2c_w}{g}F_L^c$, where F_L^c is one of the form factors defined in (6) of Ref. [44], which in turn can be shown to vanish. The assumptions in Ref. [44] are (i) the standard seesaw mechanism with ultra-heavy right neutrinos, (ii) no charged wino or Higgsino mixing, and (iii) the dominance of the wino contribution. Under these three assumptions, the interaction vertices occurring in the form factor $F_{l'lZ}^{L,\tilde{N}}$ simplify as follows:

$$\tilde{B}_{lmA}^{R,1}, \tilde{B}_{lmA}^{R,2} \rightarrow -U_{lk},$$

$$\tilde{C}_{AB}^1, \tilde{C}_{AB}^2, \tilde{C}_{AB}^3, \tilde{C}_{AB}^4 \rightarrow -\frac{1}{2}\delta_{kk'}, \qquad V_{mk}^{\tilde{\chi}^- R} \rightarrow c_w^2, \tag{4.6}$$

where A, B assume now the restricted range of values k, $k' = 1, 2, 3$ and U is a 3×3 unitary matrix. Given the simplifications in (4.6), we recover the expression of Ref. [44], resulting in the replacement: $F_{l'lZ}^{L,\tilde{N}} \rightarrow \frac{2c_w}{g}F_L^c$. The above nontrivial checks provide firm support for the correctness of our analytical and numerical results that we have presented in this section.

V. CONCLUSIONS

We have analyzed charged lepton flavor violation in the MSSM extended by low-scale singlet heavy neutrinos, paying special attention to the individual loop contributions due to the heavy neutrinos $N_{1,2,3}$, sneutrinos $\tilde{N}_{1,2,...,12}$ and soft SUSY-breaking terms. In our analysis, we have

included for the first time the complete set of box diagrams, in addition to the photon and the Z-boson-mediated interactions. We have also derived the complete set of chiral amplitudes and their associate form factors related to the neutrinoless three-body CLFV decays of the muon and tau, such as $\mu \rightarrow eee$, $\tau \rightarrow \mu\mu\mu$, $\tau \rightarrow e\mu\mu$ and $\tau \rightarrow ee\mu$, and to the coherent $\mu \rightarrow e$ conversion in nuclei. Our analytical results are general and can be applied to most of the new physics models with CLFV. In this context, we emphasize that our systematic analysis has revealed the existence of two new box form factors, which have not been considered before in the existing literature of new physics theories with CLFV.

Our detailed study has shown that the soft SUSY-breaking effects in the Z-boson-mediated graphs dominate the CLFV observables, for appreciable regions of the ν_RMSSM parameter space in mSUGRA. Nevertheless, there is a significant portion of parameter space for heavy neutrino masses $m_N \lesssim 1$ TeV, where box diagrams involving heavy neutrinos in the loop can be comparable to, or even larger than the corresponding Z-boson-exchange diagrams in $\mu \rightarrow eee$ and in $\mu \rightarrow e$ conversion in nuclei (cf. Fig. 11). In the same kinematic regime, due to accidental cancellations, we have also observed a suppression of the branching ratios for the photonic CLFV decays $\mu \rightarrow e\gamma$, as well as for the decays $\tau \rightarrow e\gamma$ and $\tau \rightarrow \mu\gamma$. As mentioned in the Introduction, such a suppression in low-scale seesaw models is a consequence of a cancellation between particle and sparticle contributions due to the approximate realization of the SUSY no-go theorem due to Ferrara and Remiddi [43]. Instead, in high-scale seesaw models such cancellations can only occur for particular choices of the neutrino Yukawa and Majorana mass textures [39,52]. Hence, the results obtained within supersymmetric low-scale seesaw type-I models, with $m_N \lesssim 10$ TeV, corroborate the original findings in Ref. [34], where the usual paradigm with the photon dipole-moment operators dominating the CLFV observables in high-scale seesaw models [37,38] gets radically modified, such that $\mu \rightarrow eee$ and $\mu \rightarrow e$ conversion may also represent sensitive probes of CLFV.

We have found that unlike heavy neutrinos, CLFV effects induced by sneutrinos remain subdominant for the entire region of the mSUGRA parameter space. In addition, the perturbativity constraint on the neutrino Yukawa couplings $\mathbf{h}_\nu$ up to the GUT scale renders the quartic coupling contributions of order $(\mathbf{h}_\nu)^4$ small. The present study has focused on providing numerical predictions for relatively small and intermediate values of $\tan\beta$, i.e. $\tan\beta \lesssim 20$, where neutral Higgs-mediated interactions constrained by the recent LHCb observation of the decay $B_s \rightarrow \mu\mu$ are not expected to give sizeable contributions. A global analysis that includes large $\tan\beta$ effects on CLFV observables and LHC constraints will be given in a forthcoming communication.

APPENDIX A: INTERACTION VERTICES

In this appendix, we list the Lagrangians describing the interaction vertices required to calculate the transition amplitudes for the CLFV processes under study. The corresponding interaction vertices for the SM and the MSSM are obtained by adopting the conventions of the public code FeynArts-3.3. FVMSSM.mod. The Lagrangians of interest to us include

(1) Vertices from 2HDM sector of the MSSM involving SM particles only,

$$\mathcal{L}_{\bar{d}uH^-} + \text{H.c.} = \frac{g_w}{\sqrt{2}M_W} V_{ij}^* \bar{d}_j (t_\beta m_{d_j} P_L$$
$$+ t_\beta^{-1} m_{u_i} P_R) u_i H^- + \text{H.c.} \quad (A1)$$

Here H^- is the negatively charged Higgs scalar, V is the Cabibbo-Kobayashi-Maskawa matrix, m_{d_i} and m_{u_i} are the quark masses and $c_w = \cos\theta_w$.

(2) Vertices of singlet neutrinos in the ν_RSM sector of the MSSM,

$$\mathcal{L}_{\bar{e}nG^-} + \text{H.c.} = \frac{g_w}{\sqrt{2}M_W} B_{ia} \bar{e}_i (-m_{e_i} P_L + m_{n_a} P_R) n_a G^-$$
$$+ \text{H.c.}, \quad (A2)$$

$$\mathcal{L}_{\bar{e}nW^-} + \text{H.c.} = -\frac{g_w}{\sqrt{2}} B_{ia} \bar{e}_i \gamma^\mu P_L n_a W_\mu^- + \text{H.c.}, \quad (A3)$$

$$\mathcal{L}_{\bar{n}nZ} = -\frac{g_w}{2c_W} C_{ab} \bar{n}_a \gamma^\mu P_L n_b Z_\mu. \quad (A4)$$

Here n_a and m_{n_a} denote the neutrino mass eigenstates and their respective masses and B and C are lepton flavor mixing matrices defined in Refs. [29,33]. The matrices B and C satisfy the following set of relations:

$$B_{la} B_{l'a}^* = \delta_{ll'}, \quad C_{ac} C_{bc} = C_{ab}, \quad B_{lb} C_{ba} = B_{la},$$
$$B_{la}^* B_{lb} = C_{ab}, \quad m_a C_{ac} C_{b\bar{c}} = 0, \quad m_a B_{lb} C_{ba}^* = 0,$$
$$m_a B_{la} B_{l'a} = 0. \quad (A5)$$

(3) Vertices from the 2HDM sector of the MSSM involving Majorana neutrinos,

$$\mathcal{L}_{\bar{e}nH^-} + \text{H.c.} = \frac{g_w}{\sqrt{2}M_W} B_{ia} \bar{e}_i (t_\beta m_{e_i} P_L + t_\beta^{-1} m_{n_a} P_R)$$
$$\times n_a H^- + \text{H.c.} \quad (A6)$$

(4) MSSM vertices with sparticles,

$$\mathcal{L}_{\bar{d}\tilde{\chi}^-\tilde{u}} + \text{H.c.} = g_w \bar{d}_j (\tilde{V}_{jma}^{-dL} P_L + \tilde{V}_{jma}^{-dR} P_R) \tilde{\chi}_m^- \tilde{u}_a$$
$$+ \text{H.c.}, \quad (A7)$$

$$\mathcal{L}_{\bar{u}\tilde{\chi}^+\tilde{d}} + \text{H.c.} = g_w \bar{u}_j (\tilde{V}_{jma}^{+uL} P_L + \tilde{V}_{jma}^{+uL} P_R) \tilde{\chi}_m^+ \tilde{d}_a$$
$$+ \text{H.c.}, \quad (A8)$$

$$\mathcal{L}_{\overline{\tilde{\chi}^-}\tilde{\chi}^-A} + \mathcal{L}_{\overline{\tilde{\chi}^+}\tilde{\chi}^+A} = e \overline{\tilde{\chi}_m^-} \gamma^\mu \tilde{\chi}_m^- A_\mu - e \overline{\tilde{\chi}_m^+} \gamma^\mu \tilde{\chi}_m^+ A_\mu, \quad (A9)$$

$$\mathcal{L}_{\overline{\tilde{\chi}^-}\tilde{\chi}^-Z} + \mathcal{L}_{\overline{\tilde{\chi}^+}\tilde{\chi}^+Z}$$
$$= \frac{g_w}{c_W} \overline{\tilde{\chi}_m^-} \gamma^\mu (V_{mk}^{\tilde{\chi}^-L} P_L + V_{mk}^{\tilde{\chi}^-R} P_R) \tilde{\chi}_k^- Z_\mu$$
$$- \frac{g_w}{c_W} \overline{\tilde{\chi}_m^+} \gamma^\mu (V_{mk}^{\tilde{\chi}^-L*} P_R + V_{mk}^{\tilde{\chi}^-R*} P_L) \tilde{\chi}_k^+ Z_\mu, \quad (A10)$$

$$\mathcal{L}_{\bar{\tilde{\chi}}^0\tilde{\chi}^0Z} = \frac{g}{c_w} \bar{\tilde{\chi}}_m^0 (\gamma^\mu P_L V_{mk}^{\tilde{\chi}^0L} + \gamma^\mu P_R V_{mk}^{\tilde{\chi}^0R}) \tilde{\chi}_k^0 Z_\mu \quad (A11)$$

$$\mathcal{L}_{\tilde{e}^*\bar{e}Z} = g_w \tilde{V}_{ab}^{\tilde{e}} \tilde{e}_a^* i \overleftrightarrow{\partial}^\mu \tilde{e}_b Z_\mu, \quad (A12)$$

$$\mathcal{L}_{\bar{e}\tilde{\chi}^0\tilde{e}} + \mathcal{L}_{\overline{\tilde{\chi}^0}e\tilde{e}^*} = g_w \bar{e}_j (P_L \tilde{V}_{jma}^{0eL} + P_R \tilde{V}_{jma}^{0eR}) \tilde{\chi}^0 \tilde{e}_a$$
$$+ \text{H.c.}, \quad (A13)$$

$$\mathcal{L}_{\bar{u}\tilde{\chi}^0\tilde{u}} + \mathcal{L}_{\overline{\tilde{\chi}^0}u\tilde{u}^*} = g_w \bar{u}_j (P_L \tilde{V}_{jma}^{0uL} + P_R \tilde{V}_{jma}^{0uR}) \tilde{\chi}^0 \tilde{u}_a$$
$$+ \text{H.c.}, \quad (A14)$$

$$\mathcal{L}_{\bar{d}\tilde{\chi}^0\tilde{d}} + \mathcal{L}_{\overline{\tilde{\chi}^0}d\tilde{d}^*} = g_w \bar{d}_j (P_L \tilde{V}_{jma}^{0dL} + P_R \tilde{V}_{jma}^{0dR}) \tilde{\chi}^0 \tilde{d}_a$$
$$+ \text{H.c.}, \quad (A15)$$

where

$$\tilde{V}_{jma}^{-dL} = \frac{m_{d_j}}{\sqrt{2}c_\beta M_W} \mathcal{U}_{m2}^* V_{ij}^* (R_L^{\tilde{u}})_{ai}^*,$$
$$\tilde{V}_{jma}^{-dR} = -\mathcal{V}_{m1} V_{ij}^* (R_L^{\tilde{u}})_{ai}^* + \frac{m_{u_i}}{\sqrt{2}s_\beta M_W} \mathcal{V}_{m2} V_{ij}^* (R_R^{\tilde{u}})_{ai}^*,$$
$$(A16)$$

$$\tilde{V}_{jma}^{+uL} = \frac{m_{u_j}}{\sqrt{2}s_\beta M_W}\mathcal{V}_{m2}^* V_{ji}(R_L^{\tilde{d}})_{ai}^*,$$

$$\tilde{V}_{jma}^{+uR} = -\mathcal{U}_{m1}V_{ji}(R_L^{\tilde{d}})_{ai}^* + \frac{m_{d_i}}{\sqrt{2}c_\beta M_W}\mathcal{U}_{m2}V_{ji}(R_R^{\tilde{d}})_{ai}^*,$$

$$\text{(A17)}$$

$$V_{mk}^{\tilde{\chi}^-L} = \mathcal{U}_{m1}\mathcal{U}_{k1}^* + \frac{1}{2}\mathcal{U}_{m2}\mathcal{U}_{k2}^* - \delta_{mk}s_w^2,$$

$$V_{mk}^{\tilde{\chi}^-R} = \mathcal{V}_{m1}^*\mathcal{V}_{k1} + \frac{1}{2}\mathcal{V}_{m2}^*\mathcal{V}_{k2} - \delta_{mk}s_w^2,$$

$$\text{(A18)}$$

$$V_{mk}^{\tilde{\chi}^0L} = -\frac{1}{4}(Z_{m3}Z_{k3}^* - Z_{m4}Z_{k4}^*), \quad \text{(A19)}$$

$$V_{mk}^{\tilde{\chi}^0R} = \frac{1}{4}(Z_{m3}^*Z_{k3} - Z_{m4}^*Z_{k4}), \quad \text{(A20)}$$

$$\tilde{V}_{ab}^{\tilde{e}} = \frac{c_{2w}}{c_w}(R_L^{\tilde{e}})_{ai}(R_L^{\tilde{e}})_{bi}^* - \frac{s_w^2}{c_w}(R_R^{\tilde{e}})_{ai}(R_R^{\tilde{e}})_{bi}^*, \quad \text{(A21)}$$

$$\tilde{V}_{jma}^{0\ell L} = -\sqrt{2}t_w Z_{m1}^*(R_R^{\tilde{e}})_{aj}^* - \frac{(m_e)_j}{\sqrt{2}c_\beta M_W}Z_{m3}^*(R_L^{\tilde{e}})_{aj}^*,$$

$$\text{(A22)}$$

$$\tilde{V}_{jma}^{0\ell R} = \frac{1}{\sqrt{2}c_W}(c_W Z_{m2} + s_W Z_{m1})(R_L^{\tilde{e}})_{aj}^*$$
$$- \frac{(m_e)_j}{\sqrt{2}c_\beta M_W}Z_{m3}(R_R^{\tilde{e}})_{aj}^*, \quad \text{(A23)}$$

$$\tilde{V}_{jma}^{0uL} = \frac{2\sqrt{2}}{3}t_w Z_{m1}^*(R_R^{\tilde{u}})_{aj}^* - \frac{(m_u)_j}{\sqrt{2}s_\beta M_W}Z_{m4}^*(R_L^{\tilde{u}})_{aj}^*,$$

$$\text{(A24)}$$

$$\tilde{V}_{jma}^{0uR} = -\frac{1}{2c_W}\left(c_W Z_{m2} + \frac{1}{3}s_W Z_{m1}\right)(R_L^{\tilde{u}})_{aj}^*$$
$$- \frac{(m_u)_j}{\sqrt{2}s_\beta M_W}Z_{m4}(R_R^{\tilde{u}})_{aj}^*, \quad \text{(A25)}$$

$$\tilde{V}_{jma}^{0dL} = -\frac{\sqrt{2}}{3}t_w Z_{m1}^*(R_R^{\tilde{d}})_{aj}^* - \frac{(m_d)_j}{\sqrt{2}c_\beta M_W}Z_{m3}(R_L^{\tilde{d}})_{aj}^*,$$

$$\text{(A26)}$$

$$\tilde{V}_{jma}^{0dR} = \frac{1}{2c_W}\left(c_W Z_{m2} - \frac{1}{3}s_W Z_{m1}\right)(R_L^{\tilde{d}})_{aj}^*$$
$$- \frac{(m_d)_j}{\sqrt{2}c_\beta M_W}Z_{m3}(R_R^{\tilde{d}})_{aj}^*, \quad \text{(A27)}$$

and $c_{2w} = \cos 2\theta_w$. The unitary matrices diagonalizing the chargino mass matrix $\mathcal{U}$ and $\mathcal{V}$ and the unitary matrix diagonalizing the neutralino mass matrix Z are taken from Ref. [69]. The matrices

$$R_{ak}^{\tilde{f}L} \equiv U_{ia}^{\tilde{f}}U_{ik}^{f_L*}, \qquad R_{ak}^{\tilde{f}R} \equiv U_{i+3a}^{\tilde{f}}U_{ik}^{f_R*}, \quad \text{(A28)}$$

with $f = d, u, e$, $a = 1, 2, \ldots, 6$ and $i, k = 1, 2, 3$, quantify the disalignment between fermions and sfermions. Here U^{f_L}, U^{f_R} and $U^{\tilde{f}}$ are unitary matrices that diagonalize the fermion and sfermion mass matrices, respectively.

(5) Sneutrino vertices in the ν_RMSSM,

$$\mathcal{L}_{\tilde{e}\tilde{\chi}^-\tilde{N}} + \text{H.c.}$$
$$= g_w\tilde{N}_A\bar{\ell}_l\left(P_L\frac{m_l}{\sqrt{2}c_\beta M_W}\tilde{B}_{lmA}^{L,1} + P_R\tilde{B}_{lmA}^{R,1}\right)\tilde{\chi}_m^- + \text{H.c.}$$
$$= g_w\tilde{N}_A^*\bar{\ell}_l\left(P_L\frac{m_l}{\sqrt{2}c_\beta M_W}\tilde{B}_{lmA}^{L,2} + P_R\tilde{B}_{lmA}^{R,2}\right)\tilde{\chi}_m^- + \text{H.c.},$$

$$\text{(A29)}$$

$$\mathcal{L}_{\tilde{N}\tilde{N}Z} = \frac{g_w}{c_W}\tilde{C}_{AB}^1\tilde{N}_A^*i\overleftrightarrow{\partial}^\mu\tilde{N}_B Z_\mu$$
$$= \frac{g_w}{c_W}\tilde{C}_{AB}^2\tilde{N}_A^*i\overleftrightarrow{\partial}^\mu\tilde{N}_B^* Z_\mu$$
$$= \frac{g_w}{c_W}\tilde{C}_{AB}^3\tilde{N}_A i\overleftrightarrow{\partial}^\mu\tilde{N}_B Z_\mu$$
$$= \frac{g_w}{c_W}\tilde{C}_{AB}^4\tilde{N}_A i\overleftrightarrow{\partial}^\mu\tilde{N}_B^* Z_\mu, \quad \text{(A30)}$$

where

$$\tilde{B}_{lmA}^{L,1} = \mathcal{U}_{m2}U_{il}^{\ell_R*}\mathcal{U}_{iA}^{\tilde{\nu}},$$
$$\tilde{B}_{lmA}^{L,2} = \mathcal{U}_{m2}U_{il}^{\ell_R*}\mathcal{U}_{i+6A}^{\tilde{\nu}*},$$
$$\tilde{B}_{lmA}^{R,1} = -\mathcal{U}_{iA}^{\tilde{\nu}}U_{il}^{\ell_L*}\mathcal{V}_{m1}$$
$$\qquad + \frac{m_{n_a}}{\sqrt{2}s_\beta M_W}\mathcal{V}_{m2}\mathcal{U}_{i+9A}^{\tilde{\nu}}U_{i+3a}^{\nu*}B_{la},$$
$$\tilde{B}_{lmA}^{R,2} = -\mathcal{U}_{i+6A}^{\tilde{\nu}*}U_{il}^{\ell_L*}\mathcal{V}_{m1}$$
$$\qquad + \frac{m_{n_a}}{\sqrt{2}s_\beta M_W}\mathcal{V}_{m2}\mathcal{U}_{i+3A}^{\tilde{\nu}*}U_{i+3a}^{\nu*}B_{la},$$
$$\tilde{C}_{AB}^1 = -\frac{1}{2}\mathcal{U}_{iA}^{\tilde{\nu}*}\mathcal{U}_{iB}^{\tilde{\nu}},$$
$$\tilde{C}_{AB}^2 = -\frac{1}{2}\mathcal{U}_{iA}^{\tilde{\nu}*}\mathcal{U}_{i+6B}^{\tilde{\nu}*},$$
$$\tilde{C}_{AB}^3 = -\frac{1}{2}\mathcal{U}_{i+6A}^{\tilde{\nu}}\mathcal{U}_{iB}^{\tilde{\nu}},$$
$$\tilde{C}_{AB}^6 = -\frac{1}{2}\mathcal{U}_{i+6A}^{\tilde{\nu}}\mathcal{U}_{i+6B}^{\tilde{\nu}*}. \quad \text{(A31)}$$

In the above, $\mathcal{U}^{\tilde{\nu}}$ is the unitary matrix diagonalizing the sneutrino mass matrix.

Notice that we have factored out the weak coupling constant g_w from all interaction vertices defined above. To better identify chirality-flip mass effects in the CLFV amplitudes, we have also pulled out a factor $m_l/(\sqrt{2}c_\beta M_W)$ from the interaction vertex $\tilde{B}^L_{lmA}$.

APPENDIX B: LOOP FUNCTIONS

The CLFV amplitudes are expressed in terms of leading-order one-loop functions. We expand the loop functions with respect to the momenta and masses of the external charged leptons, while keeping only the leading nonzero terms. The leading terms may then be expressed, in terms of the dimensionless loop integrals

$$
\begin{aligned}
&\bar{J}^m_{n_1 n_2 \dots n_k}(\lambda_1, \lambda_2, \dots, \lambda_k) \\
&= \frac{(\mu^2)^{2-D/2}}{(M_W^2)^{-D/2-m+\sum_i n_i}} \int \frac{d^D\ell}{(2\pi)^D} \frac{(\ell^2)^m}{\prod_{i=1}^k (\ell^2 - m_i^2)^{n_i}} \\
&= \frac{i(-1)^{m-\sum_i n_i}}{(4\pi)^{D/2}\Gamma(\frac{D}{2})}\left(\frac{\mu^2}{M_W^2}\right)^{2-D/2} \int_0^\infty \frac{dx\, x^{D/2-1+m}}{\prod_{i=1}^k (x+\lambda_i)^{n_i}},
\end{aligned} \quad \text{(B1)}
$$

where m_i are loop particle masses, n_i are the exponents of the propagator denominators, $\lambda_i = m_i^2/M_W^2$ are dimensionless mass parameters and μ is 't Hooft's renormalization mass scale. We choose μ to be M_W, even though any other scale can be chosen equally well as a reference scale for any of the integrals. For the amplitudes we have been calculating, the integrals are either divergent and satisfy $m + 2 - \sum_i n_i = 0$, or they are convergent with $m + 2 - \sum_i n_i < 0$. For convergent integrals, we may set $D = 4$, whilst for divergent integrals we take $D = 4 - 2\varepsilon$. We pull out a factor $i/(4\pi)^2$ from all integrals. Thus, we have for finite integrals,

$$
\bar{J}^m_{n_1 n_2 \dots n_k}(\lambda_1, \lambda_2, \dots, \lambda_k) \equiv \frac{i}{(4\pi)^2} J^m_{n_1 n_2 \dots n_k}(\lambda_1, \lambda_2, \dots, \lambda_k). \quad \text{(B2)}
$$

Instead, the divergent integrals are written down as a sum of a divergent + constant term and a finite mass-dependent term:

$$
\begin{aligned}
&\bar{J}^m_{n_1 n_2 \dots n_k}(\lambda_1, \lambda_2, \dots \lambda_k) \\
&\equiv \frac{i}{(4\pi)^2}\left(\frac{1}{\varepsilon} + \text{const} + J^m_{n_1 n_2 \dots n_k}(\lambda_1, \lambda_2, \dots, \lambda_k)\right). \quad \text{(B3)}
\end{aligned}
$$

In the CLFV amplitudes, the divergent + constant terms vanish in the total sum, or as a result of a Glashow-Iliopoulos-Maiani-like mechanism. Therefore, all CLFV amplitudes can be expressed in terms of finite mass-dependent functions $J^m_{n_1 n_2 \dots}(\lambda_1, \lambda_2, \dots)$, which we call *basic integrals*. The CLFV amplitudes and the corresponding form factors considered here are described by 9 basic integrals, four for the photonic amplitude: J^0_{31}, J^1_{31}, J^1_{41} and J^2_{41}, three for the Z-boson amplitude: J^0_{11}, J^0_{111} and J^1_{111}, and two for box amplitudes: J^0_{1111} and J^1_{1111}.

APPENDIX C: ONE-LOOP FORM FACTORS

Here we present the complete analytical form of the CLFV form factors F_γ, F_Z and F_{box} defined in Sec. III, in the Feynman-'t Hooft gauge. In the following, the usual summation convention over repeated indices is implied. The interaction vertices and loop functions used here are given in Appendices A and B, respectively.

1. Photon form factors

The form factors F^L_γ, F^R_γ, G^L_γ and G^R_γ may be explicitly written as follows:

$$
\begin{aligned}
(F^L_\gamma)_{l'l} &= F^N_{l'l\gamma} + F^{L,\tilde{N}}_{l'l\gamma} + F^{L,\text{SB}}_{l'l\gamma}, \\
(F^R_\gamma)_{l'l} &= F^N_{l'l\gamma} + F^{R,\tilde{N}}_{l'l\gamma} + F^{R,\text{SB}}_{l'l\gamma}, \\
(G^L_\gamma)_{l'l} &= m_{l'}(G^N_{l'l\gamma} + G^{L,\tilde{N}}_{l'l\gamma}) + G^{L,\text{SB}}_{l'l\gamma}, \\
(G^R_\gamma)_{l'l} &= m_l(G^N_{l'l\gamma} + G^{R,\tilde{N}}_{l'l\gamma}) + G^{R,\text{SB}}_{l'l\gamma},
\end{aligned} \quad \text{(C1)}
$$

where

$$
\begin{aligned}
F^N_{l'l\gamma} &= B_{l'a}B^*_{la}\bigg[2(J^1_{31}(1, \lambda_{n_a}) - \frac{1}{6}J^2_{41}(1, \lambda_{n_a})) \\
&\quad - \frac{1}{6}\lambda_{n_a}J^2_{41}(1, \lambda_{n_a}) - \frac{1}{6t_\beta^2}\lambda_{n_a}J^2_{41}(\lambda_{H^+}, \lambda_{n_a})\bigg],
\end{aligned}
$$

$$
\begin{aligned}
G^N_{l'l\gamma} &= B_{l'a}B^*_{la}\bigg[J^1_{31}(1, \lambda_{n_a}) + J^2_{41}(1, \lambda_{n_a}) \\
&\quad + \lambda_{n_a}\left(\frac{1}{2}J^1_{41}(1, \lambda_{n_a}) - J^0_{31}(1, \lambda_{n_a})\right) \\
&\quad + \lambda_{n_a}\lambda_{H^+}\left(\frac{1}{2t_\beta^2}J^1_{41}(\lambda_{H^+}, \lambda_{n_a})\right. \\
&\quad + \left.J^0_{31}(\lambda_{H^+}, \lambda_{n_a})\right)\bigg],
\end{aligned} \quad \text{(C2)}
$$

$$F_{l'l\gamma}^{L,\tilde{N}} = \frac{1}{2}(\tilde{B}_{l'kA}^{R,1}\tilde{B}_{lkA}^{R*} + \tilde{B}_{l'kA}^{R,2}\tilde{B}_{lkA}^{R,2*})\Big[-\frac{2}{3}J_{41}^2(\lambda_{\tilde{\chi}_k}, \lambda_{\tilde{N}_A}) + \lambda_{\tilde{\chi}_k}J_{41}^1(\lambda_{\tilde{\chi}_k}, \lambda_{\tilde{N}_A})\Big],$$

$$F_{l'l\gamma}^{R,\tilde{N}} \equiv \frac{m_l m_{l'}}{4c_\beta^2 M_W^2}(\tilde{B}_{l'kA}^{L,1}\tilde{B}_{lkA}^{1*} + \tilde{B}_{l'kA}^{L,2}\tilde{B}_{lkA}^{L,2*})\Big[-\frac{2}{3}J_{41}^2(\lambda_{\tilde{\chi}_k}, \lambda_{\tilde{N}_A}) + \lambda_{\tilde{\chi}_k}J_{41}^1(\lambda_{\tilde{\chi}_k}, \lambda_{\tilde{N}_A})\Big],$$

$$G_{l'l\gamma}^{L,\tilde{N}} = \frac{1}{2}(\tilde{B}_{l'kA}^{L,1}\tilde{B}_{lkA}^{L,1*} + \tilde{B}_{l'kA}^{L,2}\tilde{B}_{lkA}^{L,2*})\Big[-\frac{m_l^2}{2c_\beta^2 M_W^2}\lambda_{\tilde{\chi}_k}J_{41}^1(\lambda_{\tilde{\chi}_k}, \lambda_{\tilde{N}_A})\Big] + \frac{1}{2}(\tilde{B}_{l'kA}^{R,1}\tilde{B}_{lkA}^{R,1*} + \tilde{B}_{l'kA}^{R,2}\tilde{B}_{lkA}^{R,2*})[-\lambda_{\tilde{\chi}_k}J_{41}^1(\lambda_{\tilde{\chi}_k}, \lambda_{\tilde{N}_A})]$$

$$+ \frac{1}{2}(\tilde{B}_{l'kA}^{\tilde{L},1}\tilde{V}_{lkA}^{R,1*} + \tilde{B}_{l'kA}^{L,2}\tilde{V}_{lkA}^{R,2*})\Big[\frac{\sqrt{2}}{c_\beta}\sqrt{\lambda_{\tilde{\chi}_k}}J_{31}^1(\lambda_{\tilde{\chi}_k}, \lambda_{\tilde{N}_A})\Big],$$

$$G_{l'l\gamma}^{R,\tilde{N}} = \frac{1}{2}(\tilde{B}_{l'kA}^{L,1}\tilde{B}_{lkA}^{L,1*} + \tilde{B}_{l'kA}^{L,2}\tilde{B}_{lkA}^{L,2*})\Big[-\frac{m_{l'}^2}{2c_\beta^2 M_W^2}\lambda_{\tilde{\chi}_k}J_{41}^1(\lambda_{\tilde{\chi}_k}, \lambda_{\tilde{N}_A})\Big] + \frac{1}{2}(\tilde{B}_{l'kA}^{R,1}\tilde{B}_{lkA}^{R,1*} + \tilde{B}_{l'kA}^{R,2}\tilde{B}_{lkA}^{R,2*})[-\lambda_{\tilde{\chi}_k}J_{41}^1(\lambda_{\tilde{\chi}_k}, \lambda_{\tilde{N}_A})]$$

$$+ \frac{1}{2}(\tilde{B}_{l'kA}^{R,1}B_{lkA}^{L,1*} + \tilde{B}_{l'kA}^{R,2}\tilde{B}_{lkA}^{L,2*})\Big[\frac{\sqrt{2}}{c_\beta}\sqrt{\lambda_{\tilde{\chi}_k}}J_{31}^1(\lambda_{\tilde{\chi}_k}, \lambda_{\tilde{N}_A})\Big], \tag{C3}$$

$$F_{l'l\gamma}^{L,\text{SB}} = \tilde{V}_{l'ma}^{0\ell R}\tilde{V}_{lma}^{0\ell R*}\Big[-\frac{1}{3}J_{41}^2(\lambda_{\tilde{e}_a}, \lambda_{\tilde{\chi}_m^0})\Big],$$

$$F_{l'l\gamma}^{R,\text{SB}} = \tilde{V}_{l'ma}^{0\ell L}\tilde{V}_{lma}^{0\ell L*}\Big[-\frac{1}{3}J_{41}^2(\lambda_{\tilde{e}_a}, \lambda_{\tilde{\chi}_m^0})\Big],$$

$$G_{l'l\gamma}^{L,\text{SB}} = \tilde{V}_{l'ma}^{0\ell R}\tilde{V}_{lma}^{0\ell R*}[m_{l'}\lambda_{\tilde{e}_a}J_{41}^1(\lambda_{\tilde{e}_a}, \lambda_{\tilde{\chi}_m^0})] + \tilde{V}_{l'ma}^{0\ell L}\tilde{V}_{lma}^{0\ell L*}[m_l\lambda_{\tilde{e}_a}J_{41}^1(\lambda_{\tilde{e}_a}, \lambda_{\tilde{\chi}_m^0})] + \tilde{V}_{l'ma}^{0\ell L}\tilde{V}_{lma}^{0\ell R*}[2m_{\tilde{\chi}_m^0}\lambda_{\tilde{e}_a}J_{31}^0(\lambda_{\tilde{e}_a}, \lambda_{\tilde{\chi}_m^0})],$$

$$G_{l'l\gamma}^{R,\text{SB}} = \tilde{V}_{l'ma}^{0\ell L}\tilde{V}_{lma}^{0\ell L*}[m_{l'}\lambda_{\tilde{e}_a}J_{41}^1(\lambda_{\tilde{e}_a}, \lambda_{\tilde{\chi}_m^0})] + \tilde{V}_{l'ma}^{0\ell R}\tilde{V}_{lma}^{0\ell R*}[m_l\lambda_{\tilde{e}_a}J_{41}^1(\lambda_{\tilde{e}_a}, \lambda_{\tilde{\chi}_m^0})] + \tilde{V}_{l'ma}^{0\ell R}\tilde{V}_{lma}^{0\ell L*}[2m_{\tilde{\chi}_m^0}\lambda_{\tilde{e}_a}J_{31}^0(\lambda_{\tilde{e}_a}, \lambda_{\tilde{\chi}_m^0})]. \tag{C4}$$

2. Z-boson form factors

The form factors F_Z^L and F_Z^R may be decomposed as follows:

$$(F_Z^L)_{l'l} = F_{l'lZ}^N + F_{l'lZ}^{L,\tilde{N}} + F_{l'lZ}^{L,\text{SB}}, \qquad (F_\gamma^R)_{l'l} = F_{l'lZ}^N + F_{l'lZ}^{R,\tilde{N}} + F_{l'lZ}^{R,\text{SB}}, \tag{C5}$$

where

$$F_{l'lZ}^{L,N} = B_{l'a}B_{la}^*\Big[\frac{5}{2}\lambda_{n_a}J_{21}^0(1, \lambda_{n_a})\Big] + B_{l'b}C_{ba}B_{la}^*\Big[-\frac{1}{2}J_{111}^0(1, \lambda_{n_b}, \lambda_{n_a}) + \frac{1}{2}\lambda_{n_a}\lambda_{n_b}J_{111}^0(1, \lambda_{n_b}, \lambda_{n_a}) + \frac{1}{2t_\beta^2}\lambda_{n_a}\lambda_{n_b}J_{111}^0(\lambda_{H^+}, \lambda_{n_b}, \lambda_{n_a})\Big],$$

$$F_{l'lZ}^{R,N} = -\frac{m_l m_{l'}t_\beta^2}{4M_W^2}B_{l'b}C_{ba}B_{la}^*J_{111}^1(\lambda_{H^+}, \lambda_{n_b}, \lambda_{n_a}), \tag{C6}$$

$$F_{l'lZ}^{L,\tilde{N}} = \frac{1}{2}(\tilde{B}_{l'mA}^{R,1}\tilde{V}_{mk}^{\tilde{\chi}^- R}\tilde{B}_{lkA}^{R,1*} + \tilde{B}_{l'mA}^{R,2}\tilde{V}_{mk}^{\tilde{\chi}^- R}\tilde{B}_{lkA}^{R,2*})J_{111}^1(\lambda_{\tilde{\chi}_m}, \lambda_{\tilde{\chi}_k}, \lambda_{\tilde{N}_A})$$

$$- (\tilde{B}_{l'mA}^{R,1}\tilde{V}_{mk}^{\tilde{\chi}^- L}\tilde{B}_{lmA}^{R,1*} + \tilde{B}_{l'mA}^{R,2}\tilde{V}_{mk}^{\tilde{\chi}^- L}\tilde{B}_{lmA}^{R,2*})\sqrt{\lambda_{\tilde{\chi}_m}\lambda_{\tilde{\chi}_k}}J_{111}^0(\lambda_{\tilde{\chi}_m}, \lambda_{\tilde{\chi}_k}, \lambda_{\tilde{N}_A})$$

$$+ \frac{1}{2}(\tilde{B}_{l'mA}^{R,1}\tilde{B}_{lkA}^{R,1*} + \tilde{B}_{l'mA}^{R,2}\tilde{B}_{lkA}^{R,2*})\Big(\frac{1}{2} - s_w^2\Big)(J_{21}^1(\lambda_{\tilde{\chi}_k}, \lambda_{\tilde{N}_A}) - 2J_{11}^0(\lambda_{\tilde{\chi}_k}, \lambda_{\tilde{N}_A})) + \frac{1}{4}(\tilde{B}_{l'kA}^{R,1}\tilde{C}_{BA}^1\tilde{B}_{lkA}^{R,1*} + \tilde{B}_{l'kA}^{R,1}\tilde{C}_{BA}^2\tilde{B}_{lkA}^{R,2*}$$

$$+ \tilde{B}_{l'mA}^{R,2}\tilde{C}_{BA}^3\tilde{B}_{lkA}^{R,1*} + \tilde{B}_{l'mA}^{R,2}\tilde{C}_{BA}^4\tilde{B}_{lkA}^{R,2*})J_{111}^1(\lambda_{\tilde{\chi}_k}, \lambda_{\tilde{N}_B}, \lambda_{\tilde{N}_A}),$$

$$F_{l'lZ}^{R,\tilde{N}} = \frac{m_l m_{l'}}{2s_\beta^2 M_W^2}\Big[\frac{1}{2}(\tilde{B}_{l'mA}^{L,1}\tilde{V}_{mk}^{\tilde{\chi}^- L}\tilde{B}_{lkA}^{L,1*} + \tilde{B}_{l'mA}^{L,2}\tilde{V}_{mk}^{\tilde{\chi}^- L}\tilde{B}_{lkA}^{L,2*})J_{111}^1(\lambda_{\tilde{\chi}_m}, \lambda_{\tilde{\chi}_k}, \lambda_{\tilde{N}_A})$$

$$- (\tilde{B}_{l'mA}^{L,1}\tilde{V}_{mk}^{\tilde{\chi}^- R}\tilde{B}_{lmA}^{L,1*} + \tilde{B}_{l'mA}^{L,2}\tilde{V}_{mk}^{\tilde{\chi}^- R}\tilde{B}_{lmA}^{L,2*})\sqrt{\lambda_{\tilde{\chi}_m}\lambda_{\tilde{\chi}_k}}J_{111}^0(\lambda_{\tilde{\chi}_m}, \lambda_{\tilde{\chi}_k}, \lambda_{\tilde{N}_A})$$

$$+ \frac{1}{2}(\tilde{B}_{l'mA}^{L,1}\tilde{B}_{lkA}^{L,1*} + \tilde{B}_{l'mA}^{L,2}\tilde{B}_{lkA}^{L,2*})(-s_w^2)(J_{21}^1(\lambda_{\tilde{\chi}_k}, \lambda_{\tilde{N}_A}) - 2J_{11}^0(\lambda_{\tilde{\chi}_k}, \lambda_{\tilde{N}_A}))$$

$$+ \frac{1}{4}(\tilde{B}_{l'kA}^{L,1}\tilde{C}_{BA}^1\tilde{B}_{lkA}^{L,1*} + \tilde{B}_{l'kA}^{L,1}\tilde{C}_{BA}^2\tilde{B}_{lkA}^{L,2*} + \tilde{B}_{l'mA}^{L,2}\tilde{C}_{BA}^3\tilde{B}_{lkA}^{L,1*} + \tilde{B}_{l'mA}^{L,2}\tilde{C}_{BA}^4\tilde{B}_{lkA}^{L,2*})J_{111}^1(\lambda_{\tilde{\chi}_k}, \lambda_{\tilde{N}_B}, \lambda_{\tilde{N}_A})\Big], \tag{C7}$$

$$F_{l'lZ}^{L,SB} = -\tilde{V}_{l'ma}^{0\ell R} \tilde{V}_{mk}^{\tilde{\chi}^0 R} \tilde{V}_{lka}^{0\ell R*} J_{111}^1(\lambda_{\tilde{\chi}_m^0}, \lambda_{\tilde{\chi}_k^0}, \lambda_{\tilde{e}_a}) + \tilde{V}_{l'ma}^{0\ell R} \tilde{V}_{mk}^{\tilde{\chi}^0 L} \tilde{V}_{lka}^{0\ell R*} 2\sqrt{\lambda_{\tilde{\chi}_m}\lambda_{\tilde{\chi}_k}} J_{111}^0(\lambda_{\tilde{\chi}_m^0}, \lambda_{\tilde{\chi}_k^0}, \lambda_{\tilde{e}_a})$$

$$+ \tilde{V}_{l'ka}^{0\ell R} \tilde{V}_{lka}^{0\ell R*}\left(\frac{1}{2} - s_w^2\right)\left(-\frac{1}{2}J_{21}^1(\lambda_{\tilde{\chi}_k^0}, \lambda_{\tilde{e}_a}) + J_{11}^0(\lambda_{\tilde{\chi}_k^0}, \lambda_{\tilde{e}_a})\right) - \frac{1}{2}\tilde{V}_{l'kb}^{0\ell L} \tilde{V}_{ba}^{\tilde{e}} \tilde{V}_{lka}^{0\ell L*} J_{111}^1(\lambda_{\tilde{\chi}_k^0}, \lambda_{\tilde{e}_b}, \lambda_{\tilde{e}_a}),$$

$$F_{l'lZ}^{R,SB} = -\tilde{V}_{l'ma}^{0\ell L} \tilde{V}_{mk}^{\tilde{\chi}^0 L} \tilde{V}_{lka}^{0\ell L*} J_{111}^1(\lambda_{\tilde{\chi}_m^0}, \lambda_{\tilde{\chi}_k^0}, \lambda_{\tilde{e}_a}) + \tilde{V}_{l'ma}^{0\ell L} \tilde{V}_{mk}^{\tilde{\chi}^0 R} \tilde{V}_{lka}^{0\ell L*} 2\sqrt{\lambda_{\tilde{\chi}_m}\lambda_{\tilde{\chi}_k}} J_{111}^0(\lambda_{\tilde{\chi}_m^0}, \lambda_{\tilde{\chi}_k^0}, \lambda_{\tilde{e}_a})$$

$$+ \tilde{V}_{l'ka}^{0\ell L} \tilde{V}_{lka}^{0\ell L*}(-s_w^2)\left(-\frac{1}{2}J_{21}^1(\lambda_{\tilde{\chi}_k^0}, \lambda_{\tilde{e}_a}) + J_{11}^0(\lambda_{\tilde{\chi}_k^0}, \lambda_{\tilde{e}_a})\right) - \frac{1}{2}\tilde{V}_{l'kb}^{0\ell R} \tilde{V}_{ba}^{\tilde{e}} \tilde{V}_{lka}^{0\ell R*} J_{111}^1(\lambda_{\tilde{\chi}_k^0}, \lambda_{\tilde{e}_b}, \lambda_{\tilde{e}_a}). \tag{C8}$$

3. Leptonic box form factors

The leptonic box amplitudes are expressed in terms of the chiral structures: $\bar{l}'\Gamma_A^X l\bar{l}_1\Gamma_A^Y l_2^C$ [cf. (3.8)]. There are two distinct contributions to the chiral amplitudes. The first one has *direct* relevance to the original structure given above and we denote it with a subscript D. The second contribution comes from a chiral amplitude of the form $\bar{l}_1\Gamma_A^X l\bar{l}'\Gamma_A^Y l_2^C$, which contributes to the original amplitude $\bar{l}'\Gamma_A^X l\bar{l}_1\Gamma_A^Y l_2^C$, after performing a Fierz transformation. This Fierz-transformed contribution is indicated with a subscript F. More explicitly, the leptonic box form factors are given by

$$B_{\ell V}^{LL} = B_{\ell V,D}^{LL} + B_{\ell V,F}^{LL}, \qquad B_{\ell V}^{RR} = B_{\ell V,D}^{RR} + B_{\ell V,F}^{RR}, \qquad B_{\ell V}^{LR} = B_{\ell V,D}^{LR} - \frac{1}{2}B_{\ell S,F}^{LR}, \qquad B_{\ell V}^{RL} = B_{\ell V,D}^{RL} - \frac{1}{2}B_{\ell S,F}^{RL},$$

$$B_{\ell S}^{LL} = B_{\ell S,D}^{LL} + \frac{1}{2}B_{\ell S,F}^{LL} + \frac{3}{2}B_{\ell T,F}^{LL}, \qquad B_{\ell S}^{RR} = B_{\ell S,D}^{RR} + \frac{1}{2}B_{\ell S,F}^{RR} + \frac{3}{2}B_{\ell T,F}^{RR}, \qquad B_{\ell S}^{LR} = B_{\ell S,D}^{LR} - 2B_{\ell V,F}^{LR}, \tag{C9}$$

$$B_{\ell S}^{RL} = B_{\ell S,D}^{RL} - 2B_{\ell V,F}^{RL}, \qquad B_{\ell T}^{LL} = B_{\ell T,D}^{LL} - \frac{1}{2}B_{\ell T,F}^{LL} + \frac{1}{2}B_{\ell S,F}^{LL}, \qquad B_{\ell T}^{RR} = B_{\ell T,D}^{RR} - \frac{1}{2}B_{\ell T,F}^{RR} + \frac{1}{2}B_{\ell S,F}^{RR}.$$

The *direct* and Fierz-transformed contributions to the form factors are related by the exchange of outgoing leptons

$$B_{\ell A,F}^{XY} = B_{\ell A,D}^{XY}(l' \leftrightarrow l_1). \tag{C10}$$

The *direct* contributions have *direct* N, SB and Fierz-transformed $\tilde{N}$ contributions:

$$B_{\ell V,D}^{LL} = B_{\ell V,D}^{LL,N} + B_{\ell V,F}^{LL,\tilde{N}} + B_{\ell V,D}^{LL,SB}, \qquad B_{\ell V,D}^{RR} = B_{\ell V,D}^{RR,SB}, \qquad B_{\ell V,D}^{LR} = B_{\ell V,D}^{LR,SB}, \qquad B_{\ell V,D}^{RL} = -\frac{1}{2}B_{\ell S,F}^{RL,\tilde{N}} + B_{\ell V,D}^{RL,SB},$$

$$B_{\ell S,D}^{LL} = B_{\ell S,D}^{LL,SB}, \qquad B_{\ell S,D}^{RR} = \frac{1}{2}B_{\ell S,F}^{RR,\tilde{N}} + B_{\ell S,D}^{RR,SB}, \qquad B_{\ell S,D}^{LR} = B_{\ell S,D}^{LR,SB}, \qquad B_{\ell S,D}^{RL} = B_{\ell S,D}^{RL,N} - 2B_{\ell V,F}^{RL,\tilde{N}} + B_{\ell S,D}^{RL,SB},$$

$$B_{\ell T,D}^{LL} = B_{\ell T,D}^{LL,SB}, \qquad B_{\ell T,D}^{RR} = \frac{1}{2}B_{\ell S,F}^{RR,\tilde{N}} + B_{\ell T,D}^{RR,SB}. \tag{C11}$$

The form factor contributions from (C11) read

$$B_{\ell V,D}^{LL,N} = B_{la}^* B_{l_2 b}^* B_{l'a} B_{l_1 b}\left[-\left(1 + \frac{\lambda_{n_a}\lambda_{n_b}}{4}\right)J_{211}^1(1, \lambda_{n_a}, \lambda_{n_b}) + 2\lambda_{n_a}\lambda_{n_b}J_{211}^0(1, \lambda_{n_a}, \lambda_{n_b}) - 2\lambda_{n_a}\lambda_{n_b}t_\beta^{-2}J_{1111}^0(1, \lambda_{H^+}, \lambda_{n_a}, \lambda_{n_b})\right.$$

$$\left. - \frac{1}{2}\lambda_a\lambda_b t_\beta^{-2}J_{1111}^1(1, \lambda_{H^+}, \lambda_{n_a}, \lambda_{n_b}) - \frac{1}{4}\lambda_a\lambda_b t_\beta^{-4}J_{211}^1(\lambda_{H^+}, \lambda_{n_a}, \lambda_{n_b})\right],$$

$$B_{\ell V,D}^{RL,N} = -B_{la}^* B_{l_2 b}^* B_{l'a} B_{l_1 b}\frac{m_l m_{l_1} t_\beta^2}{M_W^2}(J_{1111}^1(1, \lambda_{H^+}, \lambda_{n_a}, \lambda_{n_b}) + \lambda_a\lambda_b J_{1111}^0(\lambda_{H^+}, \lambda_{n_a}, \lambda_{n_b})), \tag{C12}$$

$$B_{\ell V,F}^{LL,\tilde{N}} = (\tilde{B}_{l_1 kB}^{R,1} \tilde{B}_{l_2 mB}^{R,1*} + \tilde{B}_{l_1 kB}^{R,2} \tilde{B}_{l_2 mB}^{R,2*})(\tilde{B}_{l'mA}^{R,1} \tilde{B}_{lkA}^{R,1*} + \tilde{B}_{l'mA}^{R,2} \tilde{B}_{lkA}^{R,2*})J_{1111}^1(\lambda_{\tilde{\chi}_k}, \lambda_{\tilde{\chi}_m}, \lambda_{\tilde{N}_A}, \lambda_{\tilde{N}_B}),$$

$$B_{\ell V,F}^{RL,\tilde{N}} = (\tilde{B}_{l_1 kB}^{L,1} \tilde{B}_{l_2 mB}^{R,1*} + \tilde{B}_{l_1 kB}^{L,2} \tilde{B}_{l_2 mB}^{R,2*})(\tilde{B}_{l'mA}^{R,1} \tilde{B}_{lkA}^{L,1*} + \tilde{B}_{l'mA}^{R,2} \tilde{B}_{lkA}^{L,2*})\frac{m_{l'}m_l}{2c_\beta^2 M_W^2}J_{1111}^1(\lambda_{\tilde{\chi}_k}, \lambda_{\tilde{\chi}_m}, \lambda_{\tilde{N}_A}, \lambda_{\tilde{N}_B}),$$

$$B_{\ell S,F}^{RR,\tilde{N}} = (\tilde{B}_{l_1 kB}^{R,1} \tilde{B}_{l_2 mB}^{L,1*} + \tilde{B}_{l_1 kB}^{R,2} \tilde{B}_{l_2 mB}^{L,2*})(\tilde{B}_{l'mA}^{R,1} \tilde{B}_{lkA}^{L,1*} + \tilde{B}_{l'mA}^{R,2} \tilde{B}_{lkA}^{L,2*})\frac{2m_{l_2}m_l}{c_\beta^2 M_W^2}\sqrt{\lambda_{\tilde{\chi}_k}\lambda_{\tilde{\chi}_m}} J_{1111}^0(\lambda_{\tilde{\chi}_k}, \lambda_{\tilde{\chi}_m}, \lambda_{\tilde{N}_A}, \lambda_{\tilde{N}_B}),$$

$$B_{\ell S,F}^{RL,\tilde{N}} = (\tilde{B}_{l_1 kB}^{R,1} \tilde{B}_{l_2 mB}^{R,1*} + \tilde{B}_{l_1 kB}^{R,2} \tilde{B}_{l_2 mB}^{R,2*})(\tilde{B}_{l'mA}^{L,1} \tilde{B}_{lkA}^{L,1*} + \tilde{B}_{l'mA}^{L,2} \tilde{B}_{lkA}^{L,2*})\frac{2m_{l_1}m_l}{c_\beta^2 M_W^2}\sqrt{\lambda_{\tilde{\chi}_k}\lambda_{\tilde{\chi}_m}} J_{1111}^0(\lambda_{\tilde{\chi}_k}, \lambda_{\tilde{\chi}_m}, \lambda_{\tilde{N}_A}, \lambda_{\tilde{N}_B}),$$

$$B_{\ell V,D}^{LL,\text{SB}} = -\tilde{V}_{l_1mb}^{0\ell R}\tilde{V}_{lma}^{0\ell R*}\tilde{V}_{l'na}^{0\ell R}\tilde{V}_{l_2nb}^{0\ell R*}J_{1111}^1(\lambda_{\tilde{\chi}_m^0},\lambda_{\tilde{\chi}_n^0},\lambda_{\tilde{e}_a},\lambda_{\tilde{e}_b}) - 2\tilde{V}_{l_2mb}^{0\ell R}\tilde{V}_{lma}^{0\ell R*}\tilde{V}_{l'na}^{0\ell R}\tilde{V}_{l_1nb}^{0\ell R*}\sqrt{\lambda_{\tilde{\chi}_m^0}\lambda_{\tilde{\chi}_k^0}}J_{1111}^0(\lambda_{\tilde{\chi}_m^0},\lambda_{\tilde{\chi}_n^0},\lambda_{\tilde{e}_a},\lambda_{\tilde{e}_b}),$$

$$B_{\ell V,D}^{RR,\text{SB}} = -\tilde{V}_{l_1mb}^{0\ell L}\tilde{V}_{lma}^{0\ell L*}\tilde{V}_{l'na}^{0\ell L}\tilde{V}_{l_2nb}^{0\ell L*}J_{1111}^1(\lambda_{\tilde{\chi}_m^0},\lambda_{\tilde{\chi}_n^0},\lambda_{\tilde{e}_a},\lambda_{\tilde{e}_b}) - 2\tilde{V}_{l_2mb}^{0\ell L}\tilde{V}_{lma}^{0\ell L*}\tilde{V}_{l'na}^{0\ell L}\tilde{V}_{l_1nb}^{0\ell L*}\sqrt{\lambda_{\tilde{\chi}_m^0}\lambda_{\tilde{\chi}_k^0}}J_{1111}^0(\lambda_{\tilde{\chi}_m^0},\lambda_{\tilde{\chi}_n^0},\lambda_{\tilde{e}_a},\lambda_{\tilde{e}_b}),$$

$$B_{\ell V,D}^{LR,\text{SB}} = 2\tilde{V}_{l_1mb}^{0\ell L}\tilde{V}_{lma}^{0\ell R*}\tilde{V}_{l'na}^{0\ell R}\tilde{V}_{l_2nb}^{0\ell L*}\sqrt{\lambda_{\tilde{\chi}_m^0}\lambda_{\tilde{\chi}_k^0}}J_{1111}^0(\lambda_{\tilde{\chi}_m^0},\lambda_{\tilde{\chi}_n^0},\lambda_{\tilde{e}_a},\lambda_{\tilde{e}_b}) + \tilde{V}_{l_2mb}^{0\ell L}\tilde{V}_{lma}^{0\ell R*}\tilde{V}_{l'na}^{0\ell R}\tilde{V}_{l_1nb}^{0\ell L*}J_{1111}^1(\lambda_{\tilde{\chi}_m^0},\lambda_{\tilde{\chi}_n^0},\lambda_{\tilde{e}_a},\lambda_{\tilde{e}_b}),$$

$$B_{\ell V,D}^{RL,\text{SB}} = 2\tilde{V}_{l_1mb}^{0\ell R}\tilde{V}_{lma}^{0\ell L*}\tilde{V}_{l'na}^{0\ell L}\tilde{V}_{l_2nb}^{0\ell R*}\sqrt{\lambda_{\tilde{\chi}_m^0}\lambda_{\tilde{\chi}_k^0}}J_{1111}^0(\lambda_{\tilde{\chi}_m^0},\lambda_{\tilde{\chi}_n^0},\lambda_{\tilde{e}_a},\lambda_{\tilde{e}_b}) + \tilde{V}_{l_2mb}^{0\ell R}\tilde{V}_{lma}^{0\ell L*}\tilde{V}_{l'na}^{0\ell L}\tilde{V}_{l_1nb}^{0\ell R*}J_{1111}^1(\lambda_{\tilde{\chi}_m^0},\lambda_{\tilde{\chi}_n^0},\lambda_{\tilde{e}_a},\lambda_{\tilde{e}_b}),$$

$$B_{\ell S,D}^{LL,\text{SB}} = -2\tilde{V}_{l_1mb}^{0\ell L}\tilde{V}_{lma}^{0\ell R*}\tilde{V}_{l'na}^{0\ell L}\tilde{V}_{l_2nb}^{0\ell R*}\sqrt{\lambda_{\tilde{\chi}_m^0}\lambda_{\tilde{\chi}_k^0}}J_{1111}^0(\lambda_{\tilde{\chi}_m^0},\lambda_{\tilde{\chi}_n^0},\lambda_{\tilde{e}_a},\lambda_{\tilde{e}_b}) - 2\tilde{V}_{l_2mb}^{0\ell R}\tilde{V}_{lma}^{0\ell R*}\tilde{V}_{l'na}^{0\ell L}\tilde{V}_{l_1nb}^{0\ell L*}\sqrt{\lambda_{\tilde{\chi}_m^0}\lambda_{\tilde{\chi}_k^0}}J_{1111}^0(\lambda_{\tilde{\chi}_m^0},\lambda_{\tilde{\chi}_n^0},\lambda_{\tilde{e}_a},\lambda_{\tilde{e}_b}),$$

$$B_{\ell S,D}^{RR,\text{SB}} = -2\tilde{V}_{l_1mb}^{0\ell R}\tilde{V}_{lma}^{0\ell L*}\tilde{V}_{l'na}^{0\ell R}\tilde{V}_{l_2nb}^{0\ell L*}\sqrt{\lambda_{\tilde{\chi}_m^0}\lambda_{\tilde{\chi}_k^0}}J_{1111}^0(\lambda_{\tilde{\chi}_m^0},\lambda_{\tilde{\chi}_n^0},\lambda_{\tilde{e}_a},\lambda_{\tilde{e}_b}) - 2\tilde{V}_{l_2mb}^{0\ell L}\tilde{V}_{lma}^{0\ell L*}\tilde{V}_{l'na}^{0\ell R}\tilde{V}_{l_1nb}^{0\ell R*}\sqrt{\lambda_{\tilde{\chi}_m^0}\lambda_{\tilde{\chi}_k^0}}J_{1111}^0(\lambda_{\tilde{\chi}_m^0},\lambda_{\tilde{\chi}_n^0},\lambda_{\tilde{e}_a},\lambda_{\tilde{e}_b}),$$

$$B_{\ell S,D}^{LR,\text{SB}} = 2\tilde{V}_{l_1mb}^{0\ell R}\tilde{V}_{lma}^{0\ell R*}\tilde{V}_{l'na}^{0\ell L}\tilde{V}_{l_2nb}^{0\ell L*}J_{1111}^1(\lambda_{\tilde{\chi}_m^0},\lambda_{\tilde{\chi}_n^0},\lambda_{\tilde{e}_a},\lambda_{\tilde{e}_b}) + 2\tilde{V}_{l_2mb}^{0\ell L}\tilde{V}_{lma}^{0\ell R*}\tilde{V}_{l'na}^{0\ell L}\tilde{V}_{l_1nb}^{0\ell R*}J_{1111}^1(\lambda_{\tilde{\chi}_m^0},\lambda_{\tilde{\chi}_n^0},\lambda_{\tilde{e}_a},\lambda_{\tilde{e}_b}),$$

$$B_{\ell S,D}^{RL,\text{SB}} = 2\tilde{V}_{l_1mb}^{0\ell L}\tilde{V}_{lma}^{0\ell L*}\tilde{V}_{l'na}^{0\ell R}\tilde{V}_{l_2nb}^{0\ell R*}J_{1111}^1(\lambda_{\tilde{\chi}_m^0},\lambda_{\tilde{\chi}_n^0},\lambda_{\tilde{e}_a},\lambda_{\tilde{e}_b}) + 2\tilde{V}_{l_2mb}^{0\ell R}\tilde{V}_{lma}^{0\ell L*}\tilde{V}_{l'na}^{0\ell R}\tilde{V}_{l_1nb}^{0\ell L*}J_{1111}^1(\lambda_{\tilde{\chi}_m^0},\lambda_{\tilde{\chi}_n^0},\lambda_{\tilde{e}_a},\lambda_{\tilde{e}_b}),$$

$$B_{\ell T,D}^{LL,\text{SB}} = -2\tilde{V}_{l_1mb}^{0\ell L}\tilde{V}_{lma}^{0\ell R*}\tilde{V}_{l'na}^{0\ell L}\tilde{V}_{l_2nb}^{0\ell R*}\sqrt{\lambda_{\tilde{\chi}_m^0}\lambda_{\tilde{\chi}_k^0}}J_{1111}^0(\lambda_{\tilde{\chi}_m^0},\lambda_{\tilde{\chi}_n^0},\lambda_{\tilde{e}_a},\lambda_{\tilde{e}_b}) + 2\tilde{V}_{l_2mb}^{0\ell R}\tilde{V}_{lma}^{0\ell R*}\tilde{V}_{l'na}^{0\ell L}\tilde{V}_{l_1nb}^{0\ell L*}\sqrt{\lambda_{\tilde{\chi}_m^0}\lambda_{\tilde{\chi}_k^0}}J_{1111}^0(\lambda_{\tilde{\chi}_m^0},\lambda_{\tilde{\chi}_n^0},\lambda_{\tilde{e}_a},\lambda_{\tilde{e}_b}),$$

$$B_{\ell T,D}^{RR,\text{SB}} = -2\tilde{V}_{l_1mb}^{0\ell R}\tilde{V}_{lma}^{0\ell L*}\tilde{V}_{l'na}^{0\ell R}\tilde{V}_{l_2nb}^{0\ell L*}\sqrt{\lambda_{\tilde{\chi}_m^0}\lambda_{\tilde{\chi}_k^0}}J_{1111}^0(\lambda_{\tilde{\chi}_m^0},\lambda_{\tilde{\chi}_n^0},\lambda_{\tilde{e}_a},\lambda_{\tilde{e}_b}) + 2\tilde{V}_{l_2mb}^{0\ell L}\tilde{V}_{lma}^{0\ell L*}\tilde{V}_{l'na}^{0\ell R}\tilde{V}_{l_1nb}^{0\ell R*}\sqrt{\lambda_{\tilde{\chi}_m^0}\lambda_{\tilde{\chi}_k^0}}J_{1111}^0(\lambda_{\tilde{\chi}_m^0},\lambda_{\tilde{\chi}_n^0},\lambda_{\tilde{e}_a},\lambda_{\tilde{e}_b}).$$

$$\tag{C14}$$

4. Semileptonic box form factors

Semileptonic form factors have only *direct* contributions, with the following N, $\tilde{N}$ and SB content:

$$B_{dV}^{LL} = B_{dV}^{LL,N} + B_{dV}^{LL,\tilde{N}} + B_{dV}^{LL,\text{SB}}, \qquad B_{uV}^{LL} = B_{uV}^{LL,N} + B_{uV}^{LL,\tilde{N}} + B_{uV}^{LL,\text{SB}}, \tag{C15}$$

and

$$B_{dA}^{XY} = B_{dA}^{XY,\text{SB}}, \qquad B_{uA}^{XY} = B_{uA}^{XY,\text{SB}}, \tag{C16}$$

for $(X, Y, A) \neq (L, L, V)$. The N and $\tilde{N}$ contributions are given by

$$B_{dV}^{LL,N} = B_{l'a}B_{la}^*(V^*)_{bd_1}(V)_{bd_2}\Big[-\Big(1+\frac{\lambda_{n_a}\lambda_{u_b}}{4}\Big)J_{211}^1(1,\lambda_{n_a},\lambda_{u_b}) + 2\lambda_{n_a}\lambda_{u_b}J_{211}^0(1,\lambda_{n_a},\lambda_{u_b}) + \frac{1}{2t_\beta^2}\lambda_{n_a}\lambda_{u_b}J_{1111}^0(1,\lambda_{H^+},\lambda_{n_a},\lambda_{u_b})$$

$$-\frac{1}{2t_\beta^2}\lambda_{n_a}\lambda_{u_b}J_{1111}^1(1,\lambda_{H^+},\lambda_{n_a},\lambda_{u_b}) - \frac{1}{4t_\beta^4}\lambda_{n_a}\lambda_{u_b}J_{211}^1(\lambda_{H^+},\lambda_{n_a},\lambda_{u_b})\Big],$$

$$B_{uV}^{LL,N} = B_{l'a}B_{la}^*(V^*)_{d_2b}(V)_{d_1b}\Big[\Big(4+\frac{\lambda_{n_a}\lambda_{d_b}}{4}\Big)J_{211}^1(1,\lambda_{n_a},\lambda_{d_b}) - 2\lambda_{n_a}\lambda_{d_b}J_{211}^0(1,\lambda_{n_a},\lambda_{d_b}) + \frac{1}{2}\lambda_{n_a}\lambda_{d_b}J_{1111}^0(1,\lambda_{H^+},\lambda_{n_a},\lambda_{d_b})$$

$$-\frac{1}{2}\lambda_{n_a}\lambda_{d_b}J_{1111}^1(1,\lambda_{H^+},\lambda_{n_a},\lambda_{d_b}) + \frac{1}{4}\lambda_{n_a}\lambda_{d_b}J_{211}^1(\lambda_{H^+},\lambda_{n_a},\lambda_{d_b})\Big], \tag{C17}$$

$$B_{dV}^{LL,\tilde{N}} = -\frac{1}{2}\tilde{V}_{d_1ka}^{-dR}\tilde{V}_{d_2ma}^{-dR*}(\tilde{V}_{lkA}^{-\ell R,1*}\tilde{V}_{l'mA}^{-\ell R,1} + \tilde{V}_{lkA}^{-\ell R,2*}\tilde{V}_{l'mA}^{-\ell R,2})J_{1111}^1(\lambda_{\lambda_{\tilde{\chi}_k}},\lambda_{\tilde{\chi}_m},\lambda_{\tilde{N}_A},\lambda_{\tilde{u}_a}),$$

$$B_{uV}^{LL,\tilde{N}} = -\tilde{V}_{u_1ka}^{-uR}\tilde{V}_{u_2ma}^{-uR*}(\tilde{V}_{lkA}^{-\ell R,1*}\tilde{V}_{l'mA}^{-\ell R,1} + \tilde{V}_{lkA}^{-\ell R,2*}\tilde{V}_{l'mA}^{-\ell R,2})\sqrt{\lambda_{\tilde{\chi}_k}\lambda_{\tilde{\chi}_m}}J_{1111}^0(\lambda_{\lambda_{\tilde{\chi}_k}},\lambda_{\tilde{\chi}_m},\lambda_{\tilde{N}_A},\lambda_{\tilde{d}_a}). \tag{C18}$$

The SB form factors $B_{dA}^{XY,\text{SB}}$ and $B_{uA}^{XY,\text{SB}}$, with $X = L, R$, $Y = L, R$ and $A = V, S, T$, are obtained from the *direct* leptonic form factors $B_{\ell A}^{XY,\text{SB}}$, by making the replacements: $\ell \to d$, $l_1 \to d$, $l_2 \to d$, $\tilde{e} \to \tilde{d}$ and $\ell \to u$, $l_1 \to u$, $l_2 \to u$, $\tilde{e} \to \tilde{u}$, in both the interaction vertices and the arguments of the J-loop functions that carry the index b in (C14).

[1] B. T. Cleveland *et al.* (Homestake Collaboration), Astrophys. J. **496**, 505 (1998); J. N. Abdurashitov *et al.* (SAGE Collaboration), Phys. Rev. C **80**, 015807 (2009); J. Hosaka *et al.* (Super-Kamiokande Collaboration), Phys. Rev. D **73**, 112001 (2006); J. P. Cravens *et al.* (Super-Kamiokande Collaboration), Phys. Rev. D **78**, 032002 (2008); B. Aharmim *et al.* (SNO Collaboration), Phys. Rev. C **72**, 055502 (2005); **81**, 055504 (2010).

[2] Y. Fukuda *et al.* (Super-Kamiokande Collaboration), Phys. Rev. Lett. **81**, 1562 (1998); J. Hosaka *et al.* (Super-Kamiokande Collaboration), Phys. Rev. D **74**, 032002 (2006); J. Ashie *et al.* (Super-Kamiokande Collaboration), Phys. Rev. D **71**, 112005 (2005).

[3] M. H. Ahn *et al.* (K2K Collaboration), Phys. Rev. D **74**, 072003 (2006); P. Adamson *et al.* (MINOS Collaboration), Phys. Rev. Lett. **101**, 131802 (2008); **101**, 221804 (2008); A. Habig *et al.* (MINOS Collaboration), Nucl. Phys. B, Proc. Suppl. **218**, 320 (2011); M. Hartz (T2K Collaboration), arXiv:1201.1846; P. Adamson *et al.* (MINOS Collaboration), Phys. Rev. Lett. **108**, 191801 (2012).

[4] S. Abe *et al.* (KamLAND Collaboration), Phys. Rev. Lett. **100**, 221803 (2008).

[5] Y. Abe *et al.* (DOUBLE-CHOOZ Collaboration), Phys. Rev. Lett. **108**, 131801 (2012); F. P. An *et al.* (DAYA-BAY Collaboration), Phys. Rev. Lett. **108**, 171803 (2012); J. K. Ahn *et al.* (RENO Collaboration), Phys. Rev. Lett. **108**, 191802 (2012).

[6] B. Pontecorvo, Zh. Eksp. Teor. Fiz. **33**, 549 (1957); Sov. Phys. JETP **6**, 429 (1957); Z. Maki, M. Nakagawa, and S. Sakata, Prog. Theor. Phys. **28**, 870 (1962).

[7] J. Adam *et al.* (MEG Collaboration), Phys. Rev. Lett. **107**, 171801 (2011).

[8] U. Bellgart *et al.* (SINDRUM Collaboration), Nucl. Phys. **B299**, 1 (1988).

[9] C. Dohmen *et al.* (SINDRUM II Collaboration), Phys. Lett. B **317**, 631 (1993).

[10] W. Bertl *et al.*, Eur. Phys. J. C **47**, 337 (2006).

[11] Y. Miyazaki *et al.* (Belle Collaboration), arXiv:1206.5595; Phys. Lett. B **699**, 251 (2011); B. Aubert *et al.* (*BABAR* Collaboration), Phys. Rev. Lett. **103**, 021801 (2009); K. Hayasaka *et al.* (Belle Collaboration), Phys. Lett. B **687**, 139 (2010); J. P. Lees *et al.* (*BABAR* Collaboration), Phys. Rev. D **81**, 111101 (2010); Y. Miyazaki *et al.* (Belle Collaboration), Phys. Lett. B **692**, 4 (2010); B. Aubert *et al.* (*BABAR* Collaboration), Phys. Rev. Lett. **104**, 151802 (2010); J. Beringer *et al.* (Particle Data Group), Phys. Rev. D **86**, 010001 (2012).

[12] B. A. Golden, Ph.D. thesis, University of California, Irvine, 2012, http://meg.web.psi.ch/docs/theses/BenThesis.pdf; J. Adam, Ph.D. thesis, ETH Zurich, 2012, http://meg.web.psi.ch/docs/theses/PhDThesis_Adam_2012.pdf.

[13] J. L. Hewett *et al.*, arXiv:1205.2671.

[14] N. Berger ($\mu 3e$ Collaboration), J. Phys. Conf. Ser. **408**, 012070 (2013).

[15] A. Kurup (COMET Collaboration), Nucl. Phys. B, Proc. Suppl. **218**, 38 (2011); R. Akhmetshin *et al.* (COMET Collaboration), http://j-parc.jp/researcher/Hadron/en/pac_1203/pdf/COMET-PhaseI-LoI.pdf.

[16] R. J. Abrams *et al.* (Mu2e Collaboration), arXiv:1211.7019; R. K. Kurschke, arXiv:1112.0242; E. C. Dukes, Nucl. Phys. B, Proc. Suppl. **218**, 32 (2011).

[17] Y. Kuno, Nucl. Phys. B, Proc. Suppl. **149**, 376 (2005); R. J. Barow, Nucl. Phys. Proc. Suppl. **218**, 44 (2011).

[18] K. Hayasaka, J. Phys. Conf. Ser. **171**, 012079 (2009).

[19] M. Bona *et al.* (SuperB Collaboration), arXiv:0709.0451. With great dismay, we have recently been informed that the SuperB project will be discontinued.

[20] For reviews, see H. P. Nilles, Phys. Rep. **110**, 1 (1984); H. Haber and G. Kane, Phys. Rep. **117**, 75 (1985).

[21] G. Aad *et al.*, Phys. Lett. B **716**, 1 (2012).

[22] S. Chatrchyan *et al.*, Phys. Lett. B **716**, 30 (2012).

[23] P. Minkowski, Phys. Lett. B **67**, 421 (1977); M. Gell-Mann, P. Ramond, and R. Slansky, in *Supergravity*, edited by D. Z. Freedman and P. van Nieuwenhuizen (North-Holland, Amsterdam, 1979); T. Yanagida, in Proceedings of the Workshop on the Unified Theory and the Baryon Number in the Universe, Tsukuba, Japan, 1979, edited by O. Sawada and A. Sugamoto (unpublished); S. L. Glashow, in *Quarks and Leptons, Cargèse 1979*, edited by M. Lévy *et al.* (Plenum, New York, 1980), p. 707; R. N. Mohapatra and G. Senjanović, Phys. Rev. Lett. **44**, 912 (1980); J. Schechter and J. W. F. Valle, Phys. Rev. D **22**, 2227 (1980).

[24] W. Konetschny and W. Kummer, Phys. Lett. B **70**, 433 (1977); J. Schechter and J. W. F. Valle, Phys. Rev. D **22**, 2227 (1980); G. Lazarides, Q. Shafi, and C. Wetterrich, Nucl. Phys. **B181**, 287 (1981); R. N. Mohapatra and G. Senjanovic, Phys. Rev. D **23**, 165 (1981); T. P. Cheng and L.-F. Li, Phys. Rev. D **22**, 2860 (1980); J. Schechter and J. W. F. Valle, Phys. Rev. D **25**, 774 (1982).

[25] R. Foot, H. Lew, F. G. He, and G. C. Joshi, Z. Phys. C **44**, 441 (1989).

[26] D. Wyler and L. Wolfenstein, Nucl. Phys. **B218**, 205 (1983).

[27] R. N. Mohapatra, Phys. Rev. Lett. **56**, 561 (1986); R. N. Mohapatra and J. W. F. Valle, Phys. Rev. D **34**, 1642 (1986); S. Nandi and U. Sarkar, Phys. Rev. Lett. **56**, 564 (1986).

[28] G. C. Branco, W. Grimus, and L. Lavoura, Nucl. Phys. **B312**, 492 (1989).

[29] A. Pilaftsis, Z. Phys. C **55**, 275 (1992); P. S. B. Dev and A. Pilaftsis, Phys. Rev. D **86**, 113001 (2012).

[30] A. Pilaftsis, Phys. Rev. Lett. **95**, 081602 (2005); A. Pilaftsis and T. E. J. Underwood, Phys. Rev. D **72**, 113001 (2005); F. F. Deppisch and A. Pilaftsis, Phys. Rev. D **83**, 076007 (2011).

[31] E. Nardi, E. Roulet, and D. Tommasini, Phys. Lett. B **327**, 319 (1994); S. Antusch, J. P. Baumann, and E. Fernández-Martinez, Nucl. Phys. **B810**, 369 (2009).

[32] S. Bergmann and A. Kagan, Nucl. Phys. **B538**, 368 (1999); F. del Aguila, J. de Blas, and M. Perez-Victoria, Phys. Rev. D **78**, 013010 (2008).

[33] A. Ilakovac and A. Pilaftsis, Nucl. Phys. **B437**, 491 (1995).

[34] A. Ilakovac and A. Pilaftsis, Phys. Rev. D **80**, 091902 (2009).

[35] A. Ilakovac and A. Pilaftsis, Nucl. Phys. Proc. Suppl. **218**, 26 (2011).

[36] F. Borzumati and A. Masiero, Phys. Rev. Lett. **57**, 961 (1986).

[37] J. Hisano, T. Moroi, K. Tobe, and M. Yamaguchi, Phys. Rev. D **53**, 2442 (1996).

[38] J. Hisano, T. Moroi, K. Tobe, M. Yamaguchi, and T. Yanagida, Phys. Lett. B **357**, 579 (1995); J. Hisano and D. Nomura, Phys. Rev. D **59**, 116005 (1999); D. F. Carvalho, J. R. Ellis, M. E. Gomez, and S. Lola, Phys. Lett. B **515**, 323 (2001); J. Hisano, M. Nagai, P. Paradisi, and Y. Shimizu, J. High Energy Phys. 12 (2009) 030.

[39] J. R. Ellis, J. Hisano, S. Lola, and M. Raidal, Nucl. Phys. **B621**, 208 (2002).

[40] C. Arina, F. Bazzocchi, N. Fornengo, J. C. Romao, and J. W. F. Valle, Phys. Rev. Lett. **101**, 161802 (2008); F. Deppisch and A. Pilaftsis, J. High Energy Phys. 10 (2008) 080; F.-X. Josse-Michaux and E. Molinaro, Phys. Rev. D **84**, 125021 (2011); H. An, P. S. B. Dev, Y. Cai, and R. N. Mohapatra, Phys. Rev. Lett. **108**, 081806 (2012); B. Dumont, G. Belanger, S. Fichet, S. Kraml, and T. Schwetz, J. Cosmol. Astropart. Phys. 09 (2012) 013.

[41] A. Pilaftsis, Phys. Rev. D **56**, 5431 (1997); A. Pilaftsis and T. E. J. Underwood, Nucl. Phys. **B692**, 303 (2004).

[42] T. Cohen, D. E. Morrissey, and A. Pierce, Phys. Rev. D **86**, 013009 (2012); M. Carena, G. Nardini, M. Quiros, and C. E. M. Wagner, J. High Energy Phys. 02 (2013) 001.

[43] S. Ferrara and E. Remiddi, Phys. Lett. **53B**, 347 (1974).

[44] M. Hirsch, F. Staub, and A. Vicente, Phys. Rev. D **85**, 113013 (2012).

[45] A. Abada, D. Das, A. Vicente, and C. Weiland, J. High Energy Phys. 09 (2012) 015.

[46] G. Aad *et al.* (ATLAS Collaboration), J. High Energy Phys. 07 (2012) 167; S. Chatrchyan *et al.* (CMS Collaboration), Phys. Rev. Lett. **109**, 171803 (2012).

[47] J. Bernabéu, A. Santamaria, J. Vidal, A. Mendez, and J. W. F. Valle, Phys. Lett. B **187**, 303 (1987); J. G. Körner, A. Pilaftsis, and K. Schilcher, Phys. Lett. B **300**, 381 (1993); J. Bernabéu, J. G. Körner, A. Pilaftsis, and K. Schilcher, Phys. Rev. Lett. **71**, 2695 (1993).

[48] F. Deppisch and J. W. F. Valle, Phys. Rev. D **72**, 036001 (2005).

[49] J. Kersten and A. Y. Smirnov, Phys. Rev. D **76**, 073005 (2007).

[50] A. Pilaftsis, Phys. Rev. D **78**, 013008 (2008).

[51] T. P. Cheng and L. F. Li, Phys. Rev. Lett. **45**, 1908 (1980).

[52] E. Arganda and M. Herrero, Phys. Rev. D **73**, 055003 (2006).

[53] H. C. Chiang, E. Oset, T. S. Kosmas, A. Faessler, and J. D. Vergados, Nucl. Phys. **A559**, 526 (1993).

[54] R. Kitano, M. Koike, and Y. Okada, Phys. Rev. D **66**, 096002 (2002).

[55] A. Ilakovac, B. A. Kniehl, and A. Pilaftsis, Phys. Rev. D **52**, 3993 (1995).

[56] R. Alonso, M. Dhen, M. B. Gavela, and T. Hambye, J. High Energy Phys. 01 (2013) 118.

[57] J. Ellis and K. A. Olive, Eur. Phys. J. C **72**, 2005 (2012).

[58] M. Carena, H. E. Haber, S. Heinemeyer, W. Hollik, C. E. M. Wagner, and G. Weiglein, Nucl. Phys. **B580**, 29 (2000).

[59] J. S. Lee, M. Carena, J. Ellis, A. Pilaftsis, and C. E. M. Wagner, Comput. Phys. Commun. **184**, 1220 (2013); **180**, 312 (2009); J. S. Lee, A. Pilaftsis, M. S. Carena, S. Y. Choi, M. Drees, J. R. Ellis, and C. E. M. Wagner, Comput. Phys. Commun. **156**, 283 (2004).

[60] S. Heinemeyer, M. J. Herrero, S. Penaranda, and A. M. Rodriguez-Sanchez, J. High Energy Phys. 05 (2011) 063.

[61] P. Chankowski and S. Pokorski, Int. J. Mod. Phys. A **17**, 575 (2002).

[62] S. Petcov, S. Profumo, Y. Takanishi, and C. Yaguna, Nucl. Phys. **B676**, 453 (2004).

[63] K. Hayasaka *et al.* (Belle Collaboration), Phys. Lett. B **687**, 139 (2010).

[64] B. Aubert *et al.* (*BABAR* Collaboration), Phys. Rev. Lett. **104**, 021802 (2010).

[65] The Mu2e Project at Fermilab: http://mu2e.fnal.gov/.

[66] Y. Mori *et al.* (The PRIME Working Group), "An Experimental Search for $\mu^- \to e^-$ Conversion Process at the Ultimate Sensitivity of the Order of 10^{-18} with PRISM", LOI-25, http://www-ps.kek.jp/jhf-np/LOIlist/LOIlist.html.

[67] The X-Project: http://projectx.fnal.gov.

[68] S. Ritt *et al.* (MEG Collaboration), Nucl. Phys. B, Proc. Suppl. **162**, 279 (2006).

[69] M. Drees, M. Goldbole, and P. Roy, *Theory and Phenomenology of Sparticles* (World Scientific, Singapore, 2004).